2

Historical and Future Changes in Streamflow and Continental Runoff: A Review

Aiguo Dai

ABSTRACT

Streamflow trends from 1948 to 2012 are statistically significant only in 55 (27.5%, 29 negative vs. 26 positive) of the world's largest 200 rivers. Continental runoff decreased slightly from 1949 to 1993, it then recovered to slightly above the 1950–1980 mean. The streamflow and runoff changes are consistent with precipitation records, and they all show decreases from 1950 to 2012 over most Africa, East and South Asia, eastern Australia, the southeast and northwest United States; but increases over Argentina and Uruguay, central and northern Australia, the central and northeast United States, most of Europe, and Russia. These changes resulted partly from the Interdecadal Pacific Oscillation (IPO) and other climate variations, with low (high) land precipitation and runoff during El Niño (La Niña) events. Under the RCP8.5 scenario, models project mean streamflow to increase in the 21st century by 5%–80% over most of Asia, northern Europe, northern and eastern North America, central and eastern Africa, southeastern and northwestern South America, and central and northern Australia; but decrease by 5%–50% over the Mediterranean region, southwestern North America and Central America, northern and southern South America, southern Africa, and southwestern and southeastern Australia. The projected change patterns in precipitation, runoff, and streamflow are similar, with a fairly constant runoff ratio during the 21st century.

2.1. INTRODUCTION

Runoff, the lateral flow of water on or below land surface, is an important water flux that is difficult to measure directly. As a result, land surface and hydrological models have been used to simulate runoff fields [e.g., *Döll et al*., 2003; *Rodell et al*., 2004; *Qian et al*., 2006). The model-simulated runoff may contain significant biases due to errors in the meteorological forcing data and model physics. Streamflow, the flow of water in streams, rivers, and other channels, integrates runoff from upstream of a river basin, and it has been monitored by stream gauges at thousands of locations around the world [*GRDC*, 2013]. Thus, historical records of streamflow provide a measure of basin-integrated runoff, and they have been used to calibrate model-simulated runoff fields [*Fekete et al*., 2002]. However, an observation-based or calibrated data set of historical monthly series of runoff fields over global land is still lacking.

Integrating all the runoff and streamflow leaving the continents, one can estimate the continental freshwater discharge (i.e., the amount of water leaving the continents) or runoff into the oceans [*Baumgartner and Reichel*, 1975; *Fekete et al*., 2002; *Dai and Trenberth*, 2002; *Dai et al*., 2009]. This continental discharge is an important part of the global water cycle [*Trenberth et al*., 2007], as the oceanic net water flux into the atmosphere is returned back into the seas, thereby maintaining a long-term balance of freshwater in the oceans. The discharge from rivers also brings large amounts of minerals and nutrients from land into the seas [e.g., Boyer *et al*., 2006]; thus it also plays a key

Department of Atmospheric and Environmental Sciences, University at Albany, SUNY, Albany, New York, USA; and National Center for Atmospheric Research (NCAR), Boulder, Colorado, USA

Terrestrial Water Cycle and Climate Change: Natural and Human-Induced Impacts, Geophysical Monograph 221, First Edition. Edited by Qiuhong Tang and Taikan Oki.

role in global biogeochemical cycles. Unlike evaporation over oceans, continental discharge occurs mainly at the mouths of world's major rivers, forcing ocean circulations regionally through changes in density [*Carton*, 1991].

Besides its important role in the climate system, continental runoff also represents the freshwater resource available to all inhabitants living on land [*Oki and Kanae*, 2006]. As world's population continues to grow, there are increasing demands for freshwater [*Bogardi et al*., 2013], and our groundwater resources are depleting [*Wada et al*., 2010]. Thus, variability and long-term changes in continental runoff are of great concern to water management, especially under a changing climate [*Vörösmarty et al*., 2000; *Oki and Kanae*, 2006; *Arnell and Lloyd-Hughes*, 2014; *Haddeland et al*., 2014; *Schewe et al*., 2014].

There are a large number of analyses of streamflow over individual river basins [e.g., *Ye et al*., 2003; *Yang et al*., 2004a,b; *Xiong and Guo*, 2004; *Krepper et al*., 2006; *Espinoza Villar et al*., 2009], countries [e.g., *Guetter and Georgakakos*, 1993; *Lettenmaier et al*., 1994; *Lins and Slack*, 1999; *Groisman et al*., 2001; *Zhang et al*., 2001; *Robson*, 2002; *Hyvärinen*, 2003; *Lindstrom and Bergstrom*, 2004; *Birsan et al*., 2005; *Shiklomanov et al*., 2006, 2007; *Piao et al*., 2010; *Giuntoli et al*., 2013], and regions [*Genta et al*., 1998; *Lammers et al*., 2001; *Cluis and Laberge*, 2001; *Groisman et al*., 2004; *Pasquini and Depetris*, 2007; *Stahl et al*., 2010]. Streamflow records for world's major rivers show large decadal to multidecadal variations, with small secular trends for most of them [*Cluis and Laberge*, 2001; *Lammers et al*., 2001; *Pekárová et al*., 2003; *Dai*, 2009; *Labat*, 2010]. Increased streamflow during the later half of the twentieth century has been reported over regions with increasing precipitation, such as many parts of the United States [*Lins and Slack*, 1999; *Groisman et al*., 2001; *Qian et al*., 2007], northern high latitudes [*Peterson et al*., 2002; *Rawlins et al*., 2006], and southeastern South America [*Genta et al*., 1998; *Pasquini and Depetris*, 2007]. Decreased streamflow was reported over many Canadian river basins during the last 30–50 yr of the twentieth century [*Zhang et al*., 2001], and in Africa, South and East Asia, southern Europe, and eastern Australia [*Dai et al*., 2009], where precipitation had decreased since around 1950. Because large dams and reservoirs were built along many of world's major rivers during the last 100 years and they can dramatically change the seasonal flow rates (e.g., by increasing winter low flow and reducing spring/summer peak flow) [*Cowell and Stoudt*, 2002; *Ye et al*., 2003; *Nilsson et al*., 2005; *Döll et al*., 2009; *Biemans et al*., 2011], trends in seasonal streamflow rates [e. g., *Lammers et al*., 2001] should be interpreted cautiously. Nevertheless, there is evidence that the rapid warming since the 1970s has caused an earlier onset of spring that induces earlier snowmelt and associated peak streamflow in the western United States [*Cayan et al*., 2001] and New England of the United States [*Hodgkins et al*., 2003] and earlier breakup of river ice in Russian Arctic rivers [*Smith*, 2000] and many Canadian rivers [*Zhang et al*., 2001].

There are also global analyses of river outflow to quantify the mean, variations, and changes in continental freshwater discharge into the oceans, although a lack of reliable, truly global data sets induces large uncertainties in such estimates [*Peel and MacMahon*, 2006]. Most earlier estimates of long-term mean continental discharge are based on interpolation of in situ gauge observations [*Marcinek*, 1964; *Baumgartner and Reichel,* 1975; *Grabs et al*., 1996; *Korzun*, 1978; *L'vovich,* 1979; *Dettinger and Diaz,* 2000]. More recent estimates use as much downstream gauge data as possible and model-simulated runoff and streamflow to estimate the contributions from the ungauged areas [*Dai and Trenberth*, 2002; *Dai et al*., 2009; *Clark et al*., 2015]. There are also other estimates using a combination of observations and model simulations [*Döll et al*., 2003; *Fekete et al*., 2000; *Fekete et al*., 2002; *Wilkinson et al*., 2014], pure model simulations [*McCabe and Wolock,* 2011; *Nijssen et al*., 2001; *Oki et al*., 2001; *Alkama et al*., 2011; *Munier et al*., 2012], or simple land surface water balance [*Syed et al*., 2009]. Since many land surface and hydrological models still have large mean biases in simulating runoff fields due to errors in the forcing data and model physics [*Rodell et al*., 2004; *Qian et al*., 2006], pure model-simulated runoff fields should be used with caution. Recent satellite observations have also been used to estimate changes in continental freshwater discharge [*Syed et al*., 2010].

Attempts to quantify long-term changes in continental discharge are relatively few, partly due to a lack of data. *Probst and Tardy* [1987, 1989] reported, based on records from only 50 major rivers (accounting for ~13% of global runoff), time series of freshwater discharge from each continent from the early twentieth century to 1980. Their results show large decadal to multidecadal variations in discharges from individual continents and an upward trend in discharge from South America. *Labat et al*. [2004] reported an increasing trend in global river discharge associated with global warming during the twentieth century based primarily on records from only 10 rivers. This increasing trend has motivated several studies to attribute the runoff increases either to increased water use efficiency by plants under rising CO_2 levels [e.g., *Gedney et al*., 2006] or land use and climate changes [*Piao et al*., 2007]. However, the result of *Labat et al.* [2004] was questioned by *Legates et al*. [2005], *Peel and McMahon* [2006], and *Dai et al*. [2009] on the basis of insufficient streamflow data and inclusion of nonclimatic changes such as human withdrawal of stream water [*Döll et al*., 2009; *Biemans et al*., 2011]. The most recent comprehensive analyses [*Milliman et al*., 2008; *Dai et al*., 2009] do not show an upward trend in global continental discharge.

Dai et al. [2009] analyzed available records of streamflow from farthest downstream stations on the 925 largest rivers that monitor ~80% of the global ocean-draining land areas and capture ~73% of the continental runoff. They found that annual discharges in about one third of the 200 largest rivers show statistically significant trends during 1948–2004, with the rivers having downward trends (45) outnumbering those with upward trends (19). Another recent analysis [*Alkama et al*., 2013] also suggests insignificant streamflow trends for most major rivers.

One of the major obstacles in estimating continental discharge is incomplete (i.e., with gaps) or very short station records of streamflow that only cover a fraction of global land areas. Several methods have been applied to account for the contribution from the unmonitored areas in estimating long-term mean discharge [e.g., *Perry et al*., 1996; *Fekete et al*., 2002; *Dai and Trenberth*, 2002], but this issue has largely been ignored in long-term change analyses performed by *Probst and Tardy* [1987, 1989] and *Labat et al*. [2004]. Since the monitored drainage areas by the stations with data vary with time, a simple summation of available streamflow records from a selected network will likely contain discontinuities. *Labat et al*. [2004] alleviated this problem by creating a complete, reconstructed time series for each river using the wavelet transform of available records. *Dai et al*. [2009] filled the data gaps using correlated streamflow data from upstream stations or from model simulations through regression, and estimated runoff from the unmonitored areas using simulated data by a land surface model forced by observation-based meteorological data.

Greenhouse gas (GHG)-induced-climate change has the potential to change runoff and alter river flow regimes, as shown in a large number of modeling studies [see *Collins et al*., 2013; *Arnell and Gosling*, 2013; *van Vliet et al*., 2013; *Koirala et al*., 2014; and references therein]. By the end of the 21st century under future GHG emissions scenarios, climate models project increased annual runoff over most land areas except some subtropical areas such as southern Europe and other regions around the Mediterranean Sea, southwestern North America and central America, southern Africa, and parts of South America, where precipitation decreases [*Collins et al*., 2013]. The increases over northern high latitudes are especially large due to large percentage increases in precipitation over these regions. As a result of the runoff changes, river mean and high flow rates are projected to increase in Asia, northern Europe, high-latitudes of North America, and decrease in southern Europe and southern North America [e.g., *Milly et al*., 2002, 2005; *Nohara et al*., 2006; *Dankers and Feyen*, 2009; *Hirabayashi et al*., 2008, 2013; *Kundzewicz et al*., 2010; *Tang and Lettenmaier*, 2012; *Davie et al*., 2013; *Dankers et al*., 2014; *Koirala et al*., 2014; *van Vliet et al*., 2013]. Further, low flow rates are also projected to increase across northern high latitudes and Asia, and decrease in Europe and South America [e.g., *Hirabayashi et al*., 2008; *Döll and Schmied*, 2012; *Arnell and Gosling*, 2013; *Koirala et al*., 2014], while the number of hydrological, agricultural, and other droughts is projected to increase in most regions of the world [*Wang*, 2005; *Sheffield and Wood*, 2008; *Dai*, 2011a, 2013a; *Prudhomme et al*., 2014; *Cook et al*., 2014]. However, there exists substantial variability in the projected changes in runoff and river discharge among the climate scenarios and among the individual models [*Collins et al*., 2013; *van Vliet et al*., 2014]. A consensus appears to be on shifts in the timing of river flow regimes where snowmelt is a key driver of the hydrological regime [*Adam et al*., 2009].

We emphasize that regional precipitation [*Dai*, 2013b] and thus regional runoff and streamflow [*Dai et al*., 2009] often show large decadal to multidecadal variations in observations and individual climate model runs resulting from internal climate variability. These internal variations are realization-dependent, and thus are not comparable between observations and model runs or among different model runs. Further, they can exhibit apparent trends in relatively short records (e.g., < 60 years) that can be easily mistaken as GHG-induced long-term changes [*Hegerl et al*., 2015]. Thus, extreme caution must be taken when comparing observed and climate model-simulated historical changes in runoff and streamflow. Furthermore, human activities, such as withdrawal or diversion of stream water, building large dams and reservoirs, and land-use changes, may induce decadal and long-term changes in streamflow. Thus, it is important to compare changes in multiple river basins and examine spatial patterns inferred by the streamflow records, since trends in individual streamflow records may be influenced by local human influences. Based on global hydrological modeling, *Döll et al*. [2009] found that long-term mean global discharge into the oceans and inland sinks has been reduced by 2.7% due to water withdrawals, and by 0.8% due to dams. However, this appears to be a major factor only for arid to semiarid river basins [*Milliman et al*., 2008], while climate forcing still predominates for most of world's large rivers [*Dai et al*., 2009].

For future projections, large internal variability, which is unpredictable by current climate models, induces large uncertainties in model-projected runoff and streamflow for specific regions and future decades. To focus only on the GHG-induced changes, many studies have used multimodel ensemble averaging to smooth out the internal variability [e.g., *Collins et al*., 2013], but for the real world and in individual model runs, the large internal variability may dominate over the GHG-induced long-term change for the next several decades over many regions. This presents a big challenge for decadal prediction of runoff and river discharge as current models are unable to predict the large unforced internal variations.

2.2. STREAMFLOW AND RUNOFF DATA

For evaluating climate models and global analyses, several global streamflow data sets have been compiled [e.g., *Perry et al*., 1996; *Grabs et al*., 1996, 2000; *Bodo*, 2001; *Dai and Trenberth*, 2002; *Dai et al*., 2009; *Hannah et al*., 2011; *GRDC*, 2013]. As a result of these efforts, global streamflow data sets are archived at and available from several data centers, including the Global Runoff Data Centre (GRDC; http://grdc.bafg.de), the National Center for Atmospheric Research (NCAR; http://dss.ucar.edu/catalogs/ranges/range550.html), and the University of New Hampshire (http://www.r-arcticnet.sr.unh.edu/v3.0/index.html). The streamflow and discharge data compiled by *Dai and Trenberth* [2002] and *Dai et al*. [2009] have also been freely available online (http://www.cgd.ucar.edu/cas/catalog/surface/dai-runoff/index.html). Nevertheless, updated streamflow data are still very difficult to obtain for many rivers in Asia and Africa. For rivers in North America, continuously updated streamflow data can be freely downloaded from the U.S. Geological Survey (http://nwis.waterdata.usgs.gov/nwis/) and Environment Canada (http://www.wsc.ec.gc.ca/applications/H2O/index-eng.cfm), but it still requires tedious efforts to obtain and process the data for all major North American rivers. Updated streamflow data for many Brazilian rivers (including the Amazon) can also be downloaded from http://hidroweb.ana.gov.br/, which is in Portuguese. Streamflow data for some rivers (e.g., Congo and Niger) in West and Central Africa were available online from the Hydrologic Cycle Observation System for West and Central Africa (AOCHYCOS; http://aochycos.ird.ne/INDEX/INDEX.HTM), but this site is no longer working.

The GRDC database, consisting of more than 9000 stations (Figs. 2.1–2.2), provides the most comprehensive streamflow data for the world. Figure 2.1 shows that stream gauges have good coverage over the Americas, Europe, Russia, Australia, and even Africa. But the coverage is poor over East and South Asia, and the record length is short or needs updates for African stations. The availability of discharge data in the GRDC database reaches a maximum with over 7000 stations in the late 1970s but then declines sharply, especially for the last couple of years (Fig. 2.2). The most recent decline is largely due to the time lag for the observations to be included in the GRDC database, but the long-term decreasing trend since around 1978 is consistent with that shown by *Shiklomanov et al*. [2002]. It results from the actual reduction in the monitoring gauges in some countries [*Shiklomanov et al*., 2002], and the increasing reluctance for many countries (e.g., in Asia and Africa) to share their streamflow data as water has become an important strategic resource [*U. Looser*, personal comm., 2014]. Also, as a WMO data center, the GRDC is limited to use data obtained only through official channels and is prohibited from gathering and distributing data from online sources [*U. Looser*, personal comm., 2014]. This delays the update of the GRDC database. Because of the lack of new data, it is difficult to update global analyses of continental discharge. such as *Dai et al*. [2009]. Efforts through United Nations agencies and other international collaborations (such as the GRDC) are urgently needed to obtain updated streamflow data from Asian, African, and many other countries for scientific research.

2.3. HISTORICAL CHANGES IN STREAMFLOW AND RUNOFF

I obtained new streamflow data from the GRDC and the other online sources mentioned in Section 2.2 for the world's 264 largest rivers, and updated the global analysis of *Dai et al*. [2009 to 2012; up to early 2014 for many large rivers]. Here, I provide an overview of the long-term (1948–2012) changes in streamflow for world's largest rivers and in global continental runoff mainly based on the results from the update done here and *Dai et al*. [2009]. Figure 2.3 shows that for many of the major rivers in North America, Europe, and South America, the streamflow record at the farthest downstream station is almost complete for 1948–2013. However, publicly available records of streamflow for many large rivers in South and East Asia, Africa, and also South America are very short (<20 yr) and thus insufficient for estimating long-term changes. I found that basin-averaged water-year (October–September) mean Palmer Drought Severity Index (PDSI) [*Dai*, 2011b], precipitation, and model-simulated runoff [from *Dai et al*., 2009, for 1948–2004 only] were often highly correlated (with correlation coefficient $r \approx 0.4$–0.9) with observed streamflow, and thus one of them (with the highest r) was used to fill the data gaps in the water-year streamflow data series through linear regression obtained over the period when both data were available. The use of October (of previous year) to September (of current year) mean increases the correlation with the October–September streamflow, as snowfall of the previous winter contributes to the streamflow in the same water year. This also minimizes the effect of dams, which have large impacts on seasonal flows but usually not on yearly flows [*Ye et al*., 2003; *Döll et al*., 2009; *Biemans et al*., 2011].

Figures 2.4–2.5 show the time series of the water-year mean streamflow at the farthest downstream station for world's 12 largest rivers from observations (thick solid line), with data gaps filled using PDSI, precipitation, or simulated runoff data as mentioned above (thin solid line). Also shown (dashed line) is the basin-averaged water-year mean precipitation anomaly (normalized by its standard deviation) from rain-gauge observations [from GPCC v6,

(a)

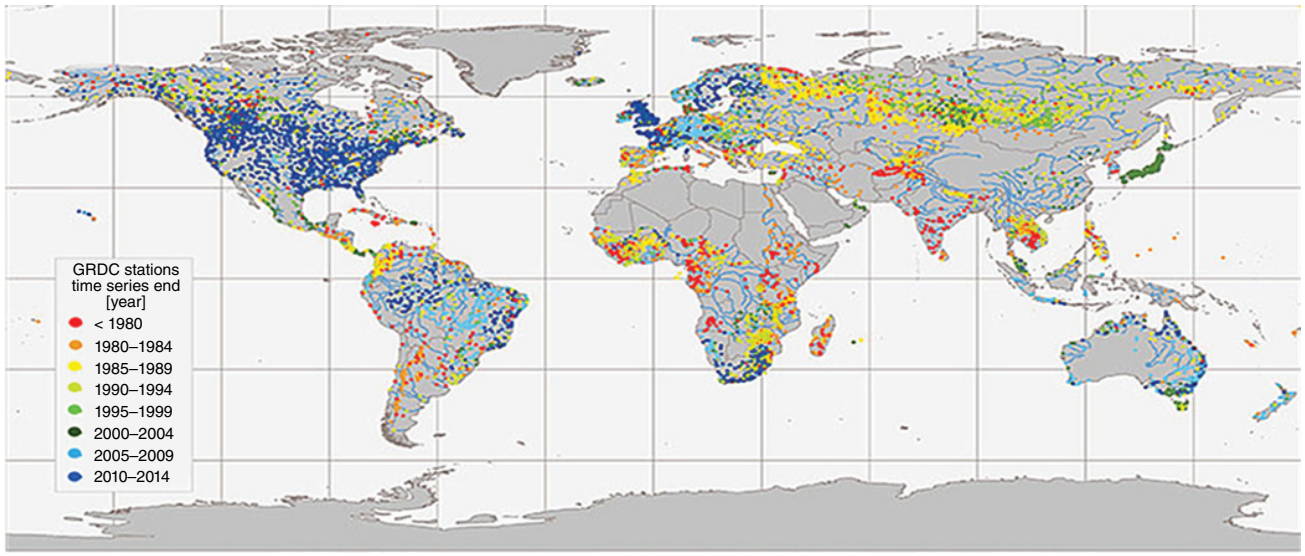

(b)

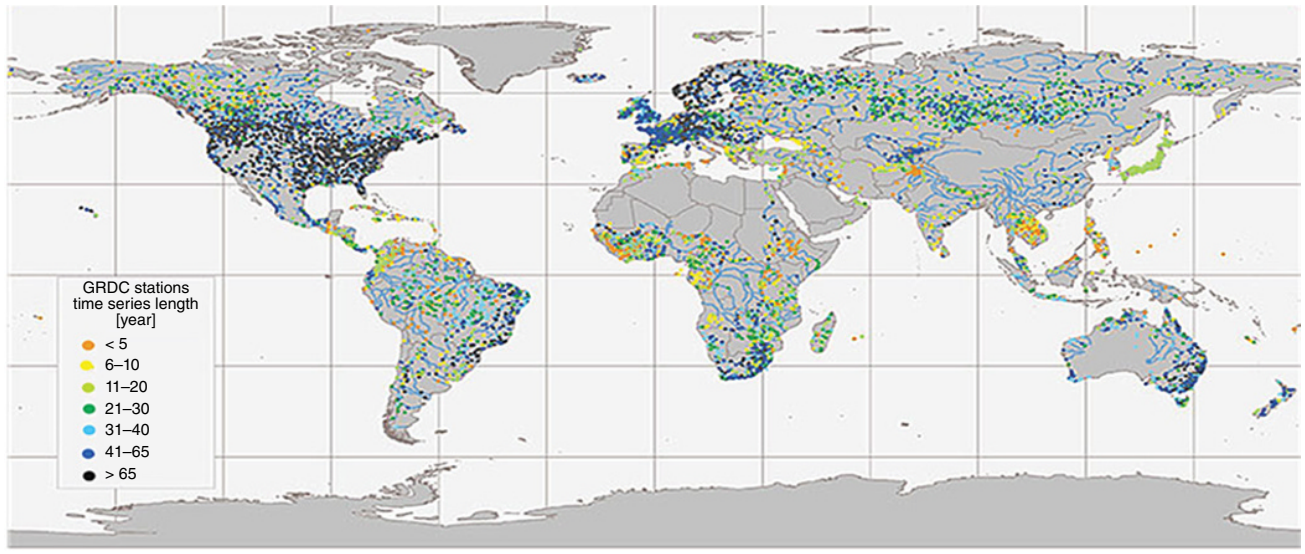

Figure 2.1 Distributions of the 9009 GRDC stations with monthly streamflow data. Colors indicate the record ending years in (a) and the record length in years in (b) (adapted from Global Runoff Data Centre, Koblenz, Germany, http://GRDC.bafg.de, used with permission).

Schneider et al., 2014; extended to 2013 with data for 2011–2013 from GPCP v2.2, *Huffman et al*., 2009].

Interannual variations and decadal and long-term changes in the observed streamflow (R) and precipitation (P) are closely correlated for most of the rivers, with r ranging from about 0.6 to 0.9. One exception is the Yenisey River, for which precipitation does not show an upward trend as in the streamflow from 1948 to 2012 (Fig. 2.5a), as noticed previously [e.g., *Adam and Lettenmaier*, 2008; *Dai*, 2009]. Figures 2.4–2.5 show that interannual and decadal variations dominate both the streamflow and precipitation series, although long-term trends are evident in some of the streamflow series, for example, for Mississippi, Yenisey, Paraná, and Lena. Decadal variations and long-term changes in runoff and precipitation are consistent with each other for most of the rivers shown in Figures 2.4–2.5. This suggests that these variations and long-term changes are likely real (i.e., not resulting from observational errors since these errors for R and P are uncorrelated) and that direct human influences on the yearly mean streamflow [e.g., through damming and withdrawal of stream water, *Döll et al*., 2009; *Biemans et al*.,

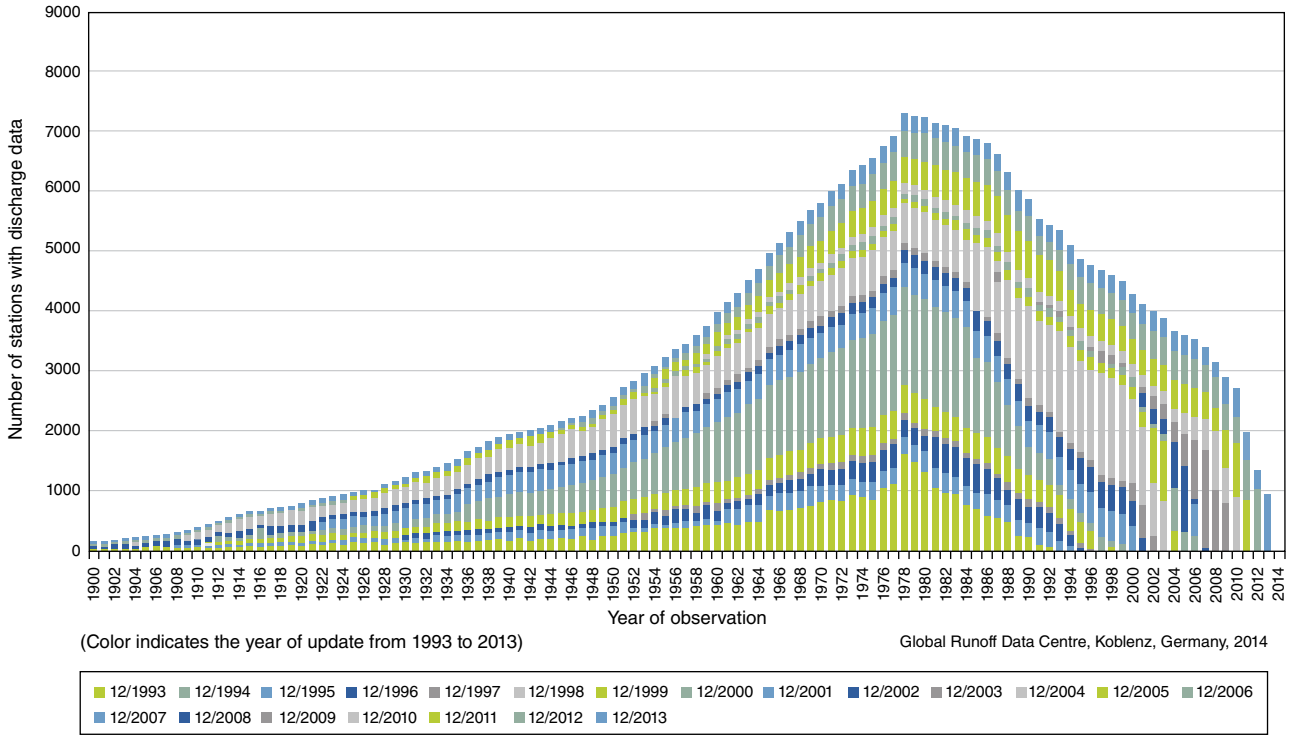

Figure 2.2 Global runoff data base, temporal distribution of river discharge data. Time series of number stations with river discharge data included in the GRDC data base as of December 2013 (Source: Global Runoff Data Centre, Koblenz, Germany, http://GRDC.bafg.de , used with permission).

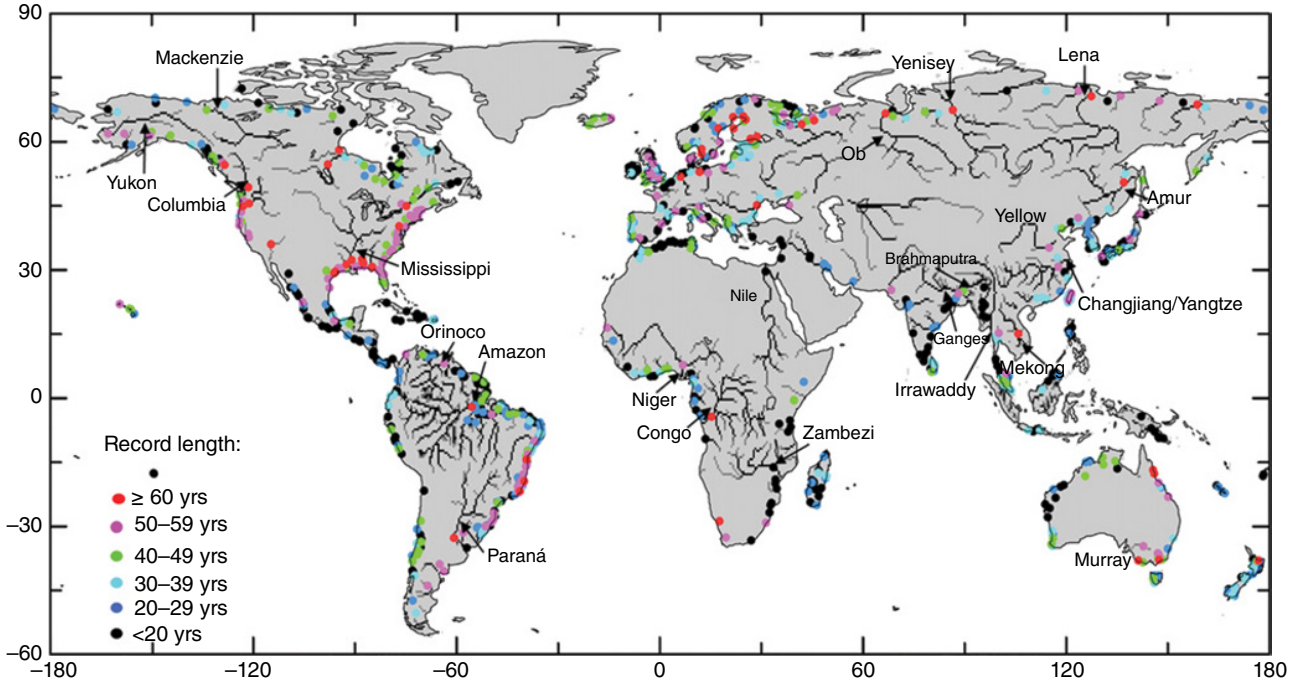

Figure 2.3 Distribution of the farthest downstream gauge stations (dots) with varying length of record of streamflow available during 1948–2013 for world's 925 largest rivers included in *Dai et al.* [2009].

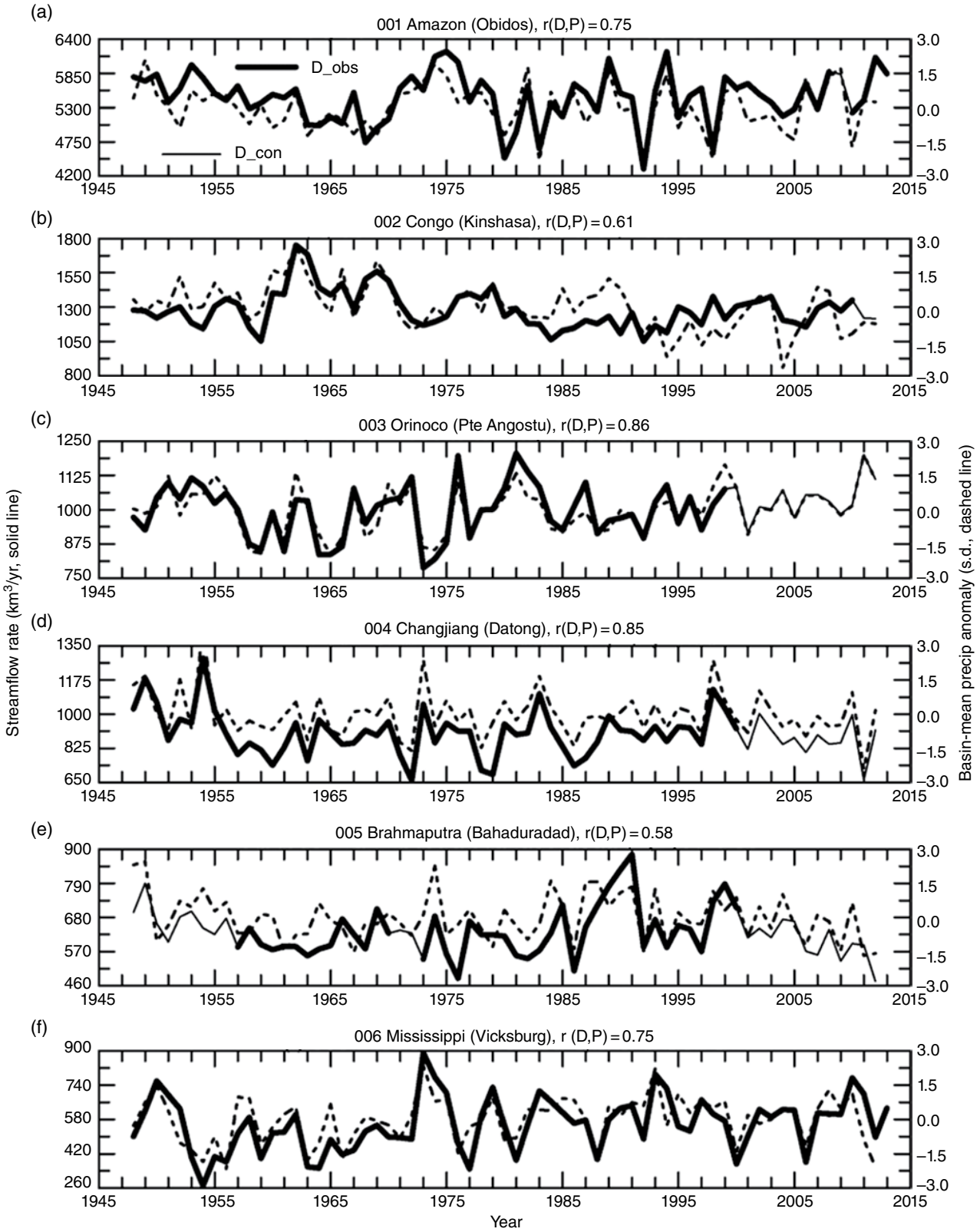

Figure 2.4 Time series of yearly (October–September) mean streamflow rate (in $km^3\ yr^{-1}$) from observations (thick solid line) and estimated using basin-mean PDSI or precipitation (thin solid line) at the farthest downstream station for world's first six largest rivers, with the river name (station name) shown on top of each panel. Also shown (dashed line) is the basin-averaged precipitation anomaly (right ordinate, normalized by its standard deviation). The correlation *r*(D,P) between the thick solid and dashed lines is also shown.

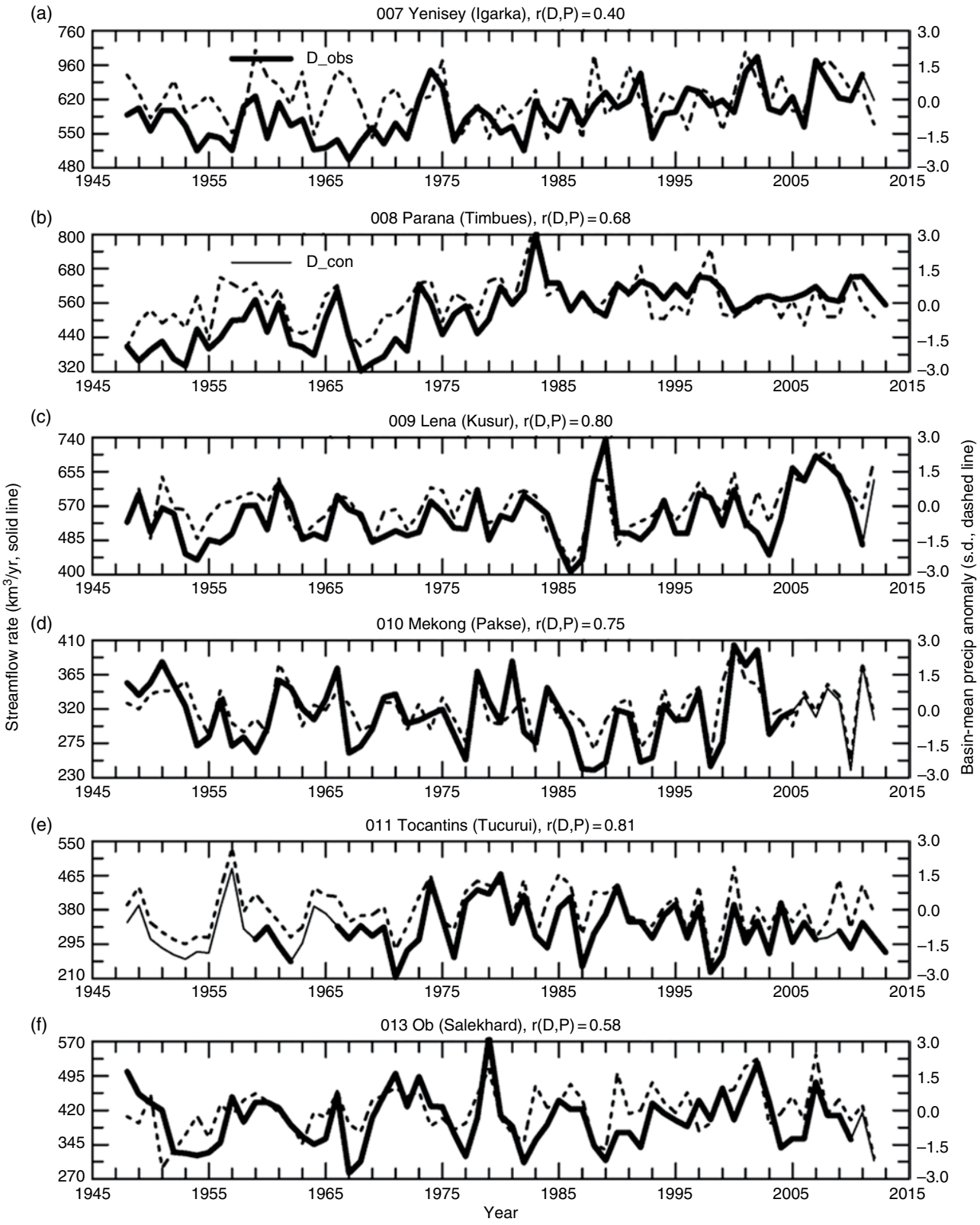

Figure 2.5 Same as Figure 2.4, but for world's next largest rivers. Time series of yearly (October–September) mean streamflow rate (in km^3 yr^{-1}) from observations (thick solid line) and estimated using basin-mean PDSI or precipitation (thin solid line) at the farthest downstream station for world's second six largest rivers, with the river name (station name) shown on top of each panel. Also shown (dashed line) is the basin-averaged precipitation anomaly (right ordinate, normalized by its standard deviation). The correlation r(D,P) between the thick solid and dashed lines is also shown.

2011] are relatively small compared with climatic forcing, a conclusion also made by *Dai et al*. [2009] for most of the world's major rivers. Substantial deviations between the R and P series do exist (Figs. 2.4–2.5), and they reflect influences on R from evapotranspiration, human activities (but only secondary compared with climatic forcing), and errors in the R and P data.

Long-term (1948–2012) trends are found to be statistically insignificant for most of world's largest rivers (Fig. 2.6). Out of the 200 largest rivers, only 55 (27.5%) show statistically significant trends, with negative trends (29) outnumbering positive trends (26). The streamflow trends do, however, show coherent spatial patterns (Fig. 2.7a) that are broadly consistent with the trend patterns of observed precipitation from 1950 to 2012 (Fig. 2.7b). Thus, these trends result mainly from changes in precipitation rather than statistical noises. In other words, they are physically meaningful although they may be statistically insignificant locally. Figure 2.7 shows that from about 1950 to 2012, precipitation and runoff have decreased over most of Africa, East and South Asia, eastern coastal Australia, the southeast and northwest United States, western and eastern Canada, and parts of Brazil, but increased over Argentina and Uruguay, central and northern Australia, the central and northeast United States, central and northern Europe and most of Russia. A large part of these regional trends likely has resulted from multidecadal internal climate variations, especially the Interdecadal Pacific Oscillation [IPO, *Dai*, 2013b; *Dong and Dai*, 2015], although the effect of global warming is likely also important [*Zhang et al*., 2007; *Gu and Adler*, 2013].

Some regional discrepancies do exist between the streamflow-inferred runoff trends and observed precipitation trends shown in Figure 2.7. For example, over the Yenisey river basin (cf. Fig. 2.3), precipitation decreased in the downstream but increased in the upstream area (Fig. 7b), which results in little change in basin-mean precipitation from around 1950 to 2012 (Fig. 2.5a). This is in contrast to increased streamflow and runoff in this basin (Fig. 2.5a and Fig. 2.7a). Other factors, including thawing of the permafrost and changes in evapotranspiration, may have contributed to the runoff increase over the Yenisey basin [*Adam and Lettenmaier*, 2008]. It is worth noting that runoff and precipitation over the other two large Russian river basins, namely the Ob and Lena (cf. Fig. 2.3), show consistent positive trends (Fig. 2.7).

Figure 2.8a shows the global continental discharge (excluding contributions from Greenland and Antarctica) as estimated by *Dai et al*. [2009] for 1949–2004 and by this study for 2005–2012. To extend the discharge series beyond 2004, I used the updated streamflow data for the largest 264 rivers to derive a yearly series of discharge from these rivers, which account for about 65% of the global discharge. This estimated discharge is highly correlated ($r = 0.91$) with that from *Dai et al*. [2009] over 1949–2004 (thick solid line in Fig. 2.8a), and thus is used to estimate the global discharge for 2005–2012 (thin solid line in Fig. 2.8a) through linear regression over 1949–2004 with the thick solid line in Fig. 2.8a. For comparison, the

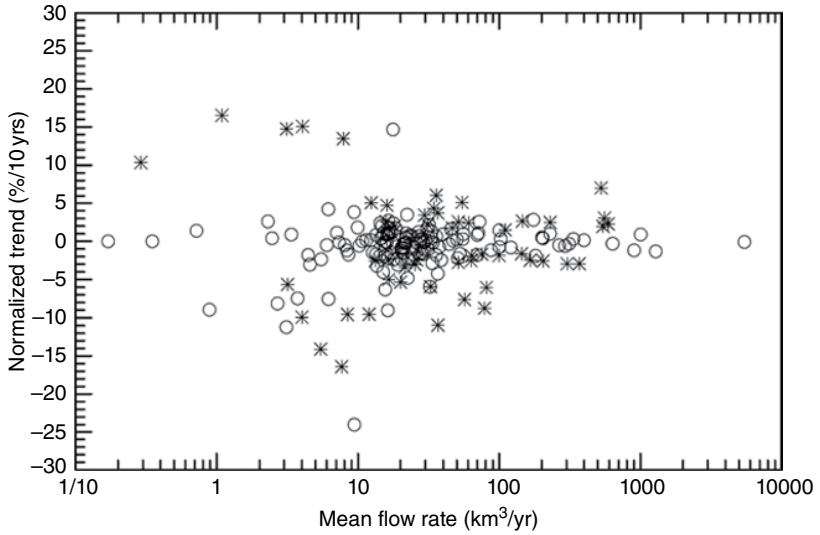

Figure 2.6 Linear trends of yearly (October–September) streamflow during 1948–2012 for world's largest 200 rivers plotted as a function of the 1948–2012 mean flow rate of the corresponding river. The trend is expressed in percentage of the mean per decade, with the statistically significant trends (at 5% level) denoted by stars and insignificant ones by open circles. Only 55 of the 200 rivers show significant trends, with 26 of them being positive and 29 being negative.

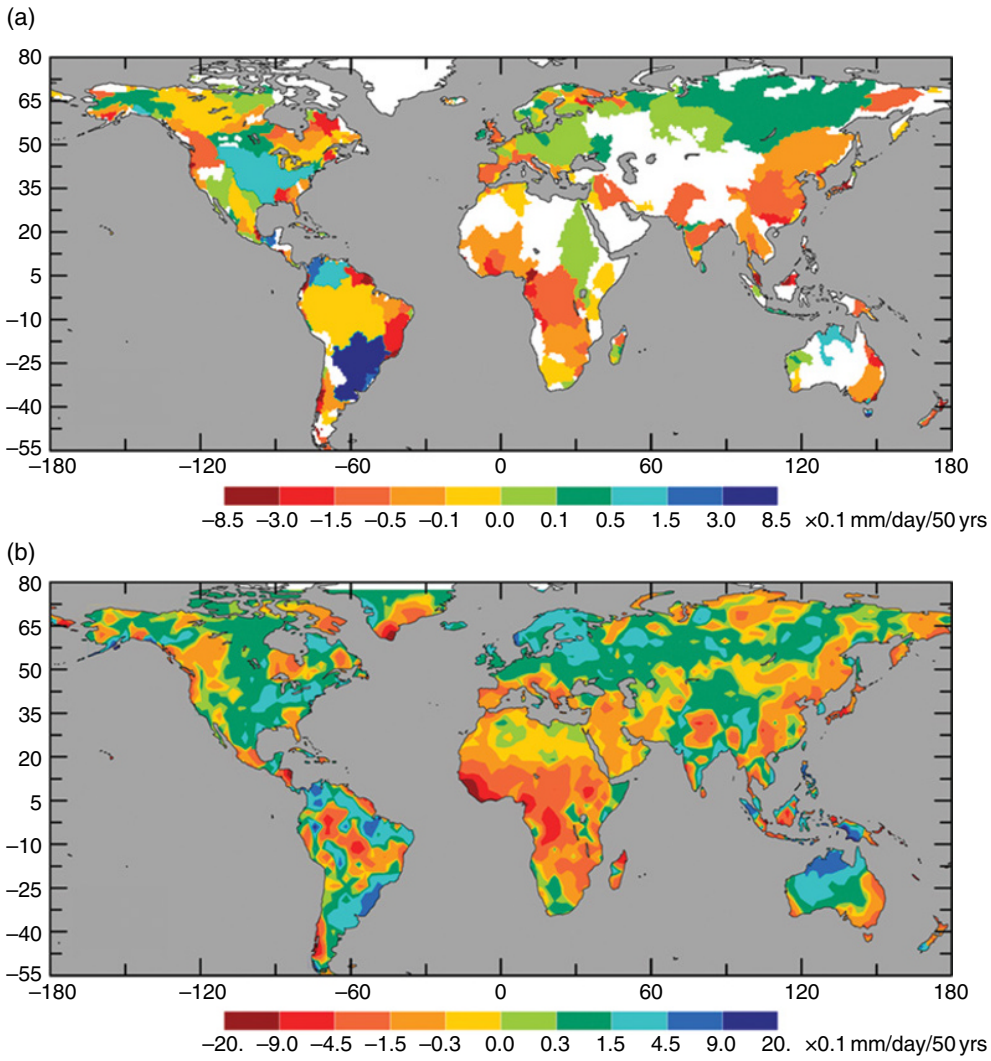

Figure 2.7 (a) Long-term (1949–2012) trends (in 0.1 mm/day per 50 years) of October–September mean runoff inferred from records of downstream river flow rates. Blank areas do not have runoff into the oceans or do not have enough observations. (b) Long-term (1950–2012) trends (in 0.1mm/day per 50 years) of annual precipitation from rain gauge observations.

October–September mean precipitation anomaly averaged over global land areas is also shown in Figure 2.8a (dashed line). Figure 2.8a shows that global continental discharge exhibits large year-to-year variations, with a weak downward trend from 1949 to 1993; thereafter, it has increased to levels slightly above those from the 1950s to 1980s. Land precipitation generally follows these decadal changes, and it also correlates with the discharge on interannual to multiyear timescales (Fig. 2.8a).

As noticed previously [e.g., *Trenberth and Dai*, 2007; *Dai et al*., 2009], both land precipitation and continental discharge are significantly correlated with the Niño3.4 (170˚W-120˚W, 5˚S-5˚N) sea surface temperature (SST) anomalies (r = −0.71 for precipitation and −0.63 for discharge), with low (high) land precipitation and continental discharge during El Niño (La Niña) events (Fig. 2.8b). During warm El Niño events, many land areas in South Asia, Australia, southern and West Africa, Central America, and northern South America usually receive below-normal precipitation, with only southern South America, the southern and central United States, and a few other land areas receiving above-normal precipitation [*Dai and Wigley*, 2000]. This results in below-normal precipitation and runoff over global land. These anomalies approximately reverse sign during cold La Niña events. Significant correlations (r = −0.50 to −0.61) were also found between the Niño3.4 SST index and the discharge into the Pacific, India, and Atlantic oceans, but not with the discharge into the Arctic Ocean and the Mediterranean and Black seas [*Dai et al*., 2009].

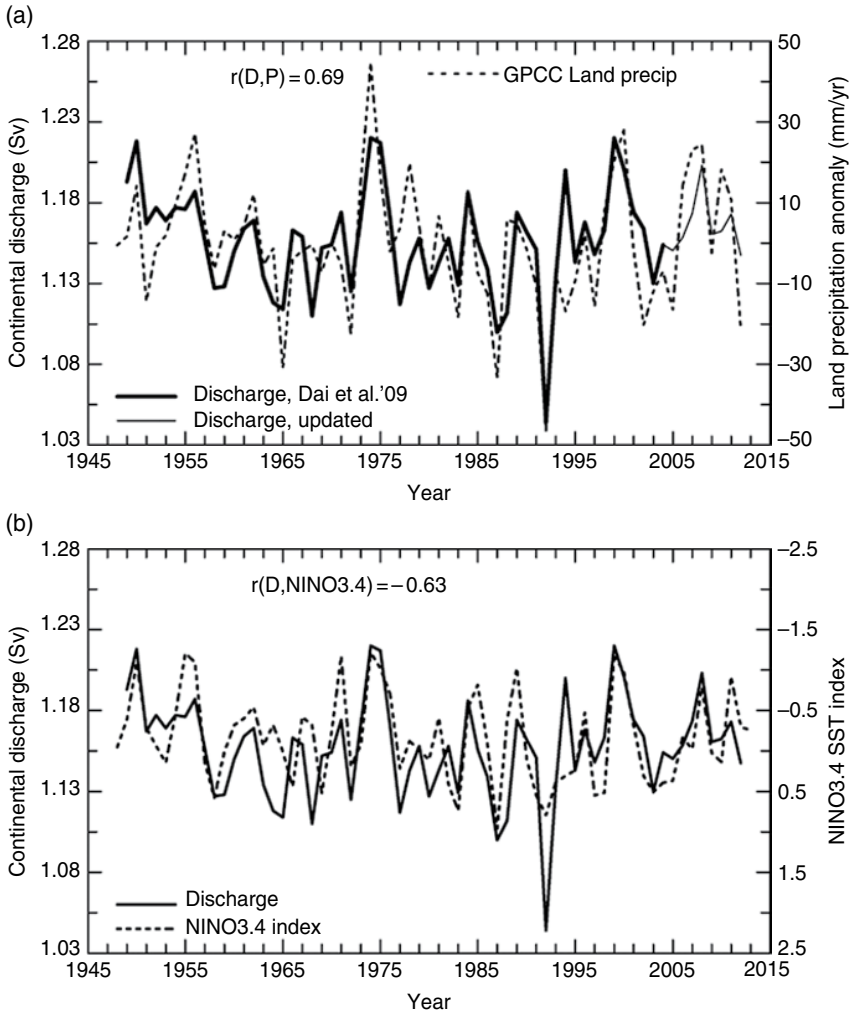

Figure 2.8 (a) Yearly time series of October–September mean total continental discharge (in Sv or 1×10^6 m^3 s^{-1}, excluding that from Greenland and Antarctica) for 1949–2004 (thick solid line) estimated based on streamflow observations from 925 world's largest rivers [from *Dai et al.*, 2009], and for 2005–2012 (thin solid line) estimated based on updated streamflow data for 264 of world's largest rivers and a linear regression with the think solid line. The dashed line is the October–September mean precipitation averaged over global (60°S–75°N) land areas. (b) Same as (a) except the dashed line is the Nino3.4 (170°W–120°W, 5°S–5°N) SST index.

Thus, El Niño-Southern Oscillation (ENSO) is a major cause for the interannual to multiyear variations in land precipitation and continental discharge. The decadal-multidecadal, low-frequency variations in the ENSO index, which are referred to as the Interdecadal Pacific Oscillations [IPO, *Dai*., 2013b], are also correlated with the decadal-multidecadal changes in land precipitation and continental discharge [Fig. 2.8; *Dong and Dai*, 2015], although the ENSO-induced interannual to multiyear variations dominate these time series. Therefore, decadal-multidecadal variations in the Pacific basin (namely the IPO) are also an important cause for decadal-multi-decadal variations in land precipitation and continental discharge.

2.4. MODEL-PROJECTED FUTURE CHANGES IN RUNOFF AND STREAMFLOW

2.4.1. Hydroclimatic Changes in the 21st Century

Before discussing future runoff and streamflow changes, we first examine model-simulated changes in precipitation and other related fields (Fig. 2.9) based on an updated analysis of *Zhao and Dai* [2015]. The change patterns shown in Fig. 2.9 are very similar to those of *Collins et al*. [2013], who showed the changes mostly in physical units instead of percentage changes. Figure 2.9a shows that under the moderate RCP4.5 emissions scenario annual precipitation (P) could increase by

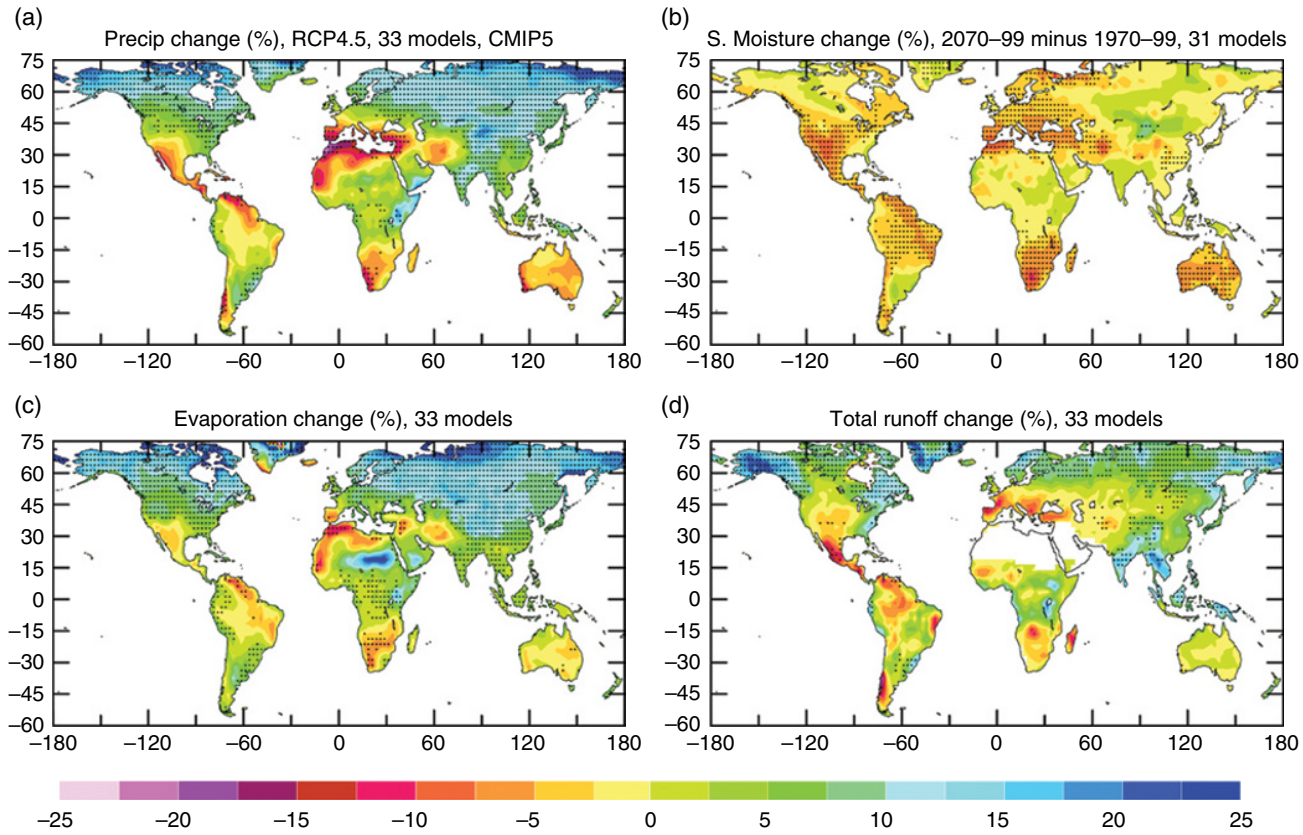

Figure 2.9 Multimodel mean long-term percentage changes from 1970–1999 to 2070–2099 (under a moderate RCP4.5 scenario) over land in annual (a) precipitation, (b) soil moisture content in the top 10 cm layer, (c) surface evapotranspiration, and (d) total runoff from 31–33 CMIP5 models. The stippling indicates at least 80% of the models agree on the sign of change. The change patterns are similar to those shown by *Collins et al.* [2013].

10%–25% from 1970–1999 to 2070–2099 over most of Eurasia, North America, and central to northern Africa, but decrease by 3%–15% over most of Australia, southern Africa, the regions around the Mediterranean, Central America, and northern South America, and southwest North America. The change patterns are similar under higher emissions scenarios except for larger magnitudes [*Collins et al.*, 2013]. The precipitation decreases over subtropical land areas are part of the larger subtropical drying zones that extend to the oceans [*Collins et al.*, 2013]. The decreases of subtropical precipitation result from both the poleward expansion of the subtropical subsidence zone [e.g., *Lu et al.*, 2007; *Scheff and Frierson*, 2012] and the increased drying by the subsidence of the Hadley circulation due to increased vertical gradient of water vapor in a warmer climate [*Chou et al.*, 2009]. The P increases in the deep tropics are mainly due to intensified moist convection [*Chou et al.*, 2009], whereas the large P increases at northern midhigh latitudes are largely due to increased water vapor content (which increases precipitation intensity) and enhanced poleward moisture transport [*Zhang et al.*, 2012] under a warmer climate.

Figure 2.9 shows that the pattern and magnitude of changes in surface evapotranspiration (ET) largely follow those for precipitation, while near-surface soil moisture (SM) decreases over most land areas, including northern Europe, most of North America, and many parts of Asia, all of which receive more precipitation. Most of the increased precipitation evaporates (Fig. 2.9c) or runs off (Fig. 2.9d), rather than being used to increase soil moisture in these areas. Besides being consistent with the increased evaporative demand [*Scheff and Frierson*, 2014; *Zhao and Dai*, 2015], the increased surface drying in spite of increased precipitation over many land areas is also consistent with the fact that most of the precipitation increase comes from increases in heavy precipitation, while the frequency of precipitation events decreases [*Trenberth et al.*, 2003; *Sun et al.*, 2007], resulting in more dry spells in a warmer climate [*Meehl et al.*, 2007].

The runoff (R) change pattern (Fig. 2.9d) roughly follows that of precipitation, with decreases over southern Africa, northern South America and Central America, southwest North America, and southern and central Europe. One exception is Australia, where precipitation

decreases but runoff does not change much, which is also shown by *Collins et al*. [2013]. This may be due to the fact that runoff is low and decoupled with precipitation, which is largely evaporated over the dry continent (so that any increases in precipitation will not result in runoff). Overall, Figures 2.9b and 2.9d seem to suggest that future agricultural drought may become more widespread while hydrological drought may increase only over limited areas. This is expected because increased evaporative demand of moisture (Fig. 2.10) by a warmer atmosphere will reduce soil-moisture content, while increased precipitation (especially intense precipitation) will lead to higher runoff in spite of more dry days. However, more detailed analyses [*Prudhomme et al*., 2014; *Zhao and Dai*, 2015] show that the frequency of hydrological drought would increase over most land areas in the 21st century despite of the increase in the mean runoff over many land areas, primarily due to the flattening of the probability distribution function of runoff in the future (*Zhao and Dai,* 2015).

The change patterns in near-surface soil moisture (Fig. 2.9b) from the CMIP5 models are similar to those of the self-calibrated Palmer Drought Severity Index with the Penman-Monteith potential evapotranspiration (sc_PDSI_pm, Fig. 2.10a) calculated off-line using the CMIP5 model output, as noticed previously by *Dai* [2013a]. Figure 2.10b shows that potential evapotranspiration (PET) calculated using the Penman-Monteith equation [*Shuttleworth*, 1993] increases everywhere over land in the 21st century by 5%–15% at low latitudes and by 10%–20% at northern mid- to high-latitudes, consistent with previous reports [*Feng and Fu*, 2013; *Scheff and Frierson*, 2014]. This leads to a reduction of 0.03–0.15 in the P/PET ratio over many land areas (Fig. 2.10c), mostly

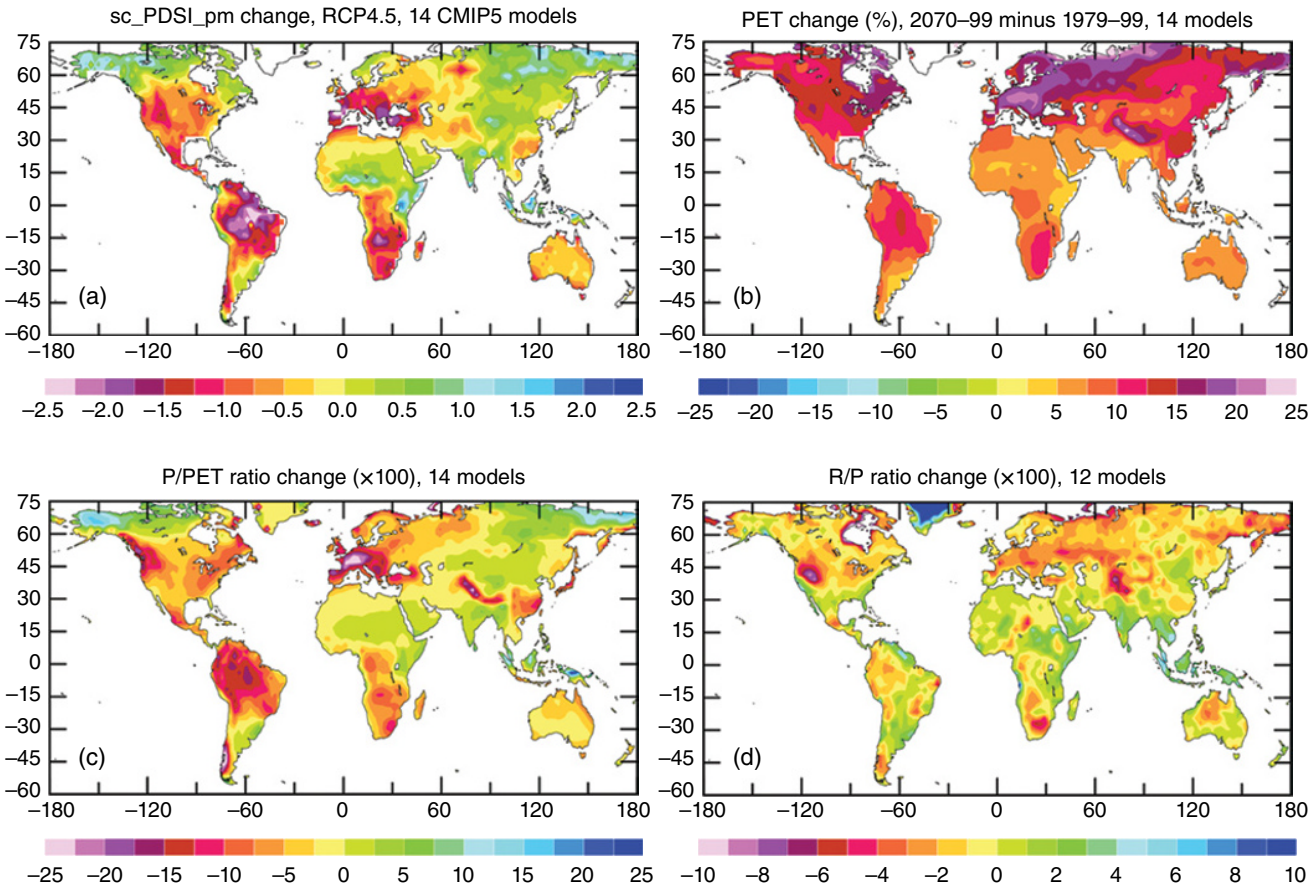

Figure 2.10 Multimodel ensemble averaged long-term changes from 1970–1999 to 2070–2099 (under the moderate RCP4.5 scenario) over land in annual (a) sc_PDSI_pm, (b) potential evapotranspiration (PET) based on the Penman-Monteith equation, (c) precipitation (P) vs. PET ratio (×100), and (d) runoff ratio (×100) estimated using data from the 14 CMIP5 models (12 for panel d). For reference, a sc_PDSI_pm value below –1 is considered drought and below –3 is considered severe to extreme drought for current climate [*Palmer*, 1965]. The sc_PDSI_pm and PET were computed for each model run and then averaged over the 14 models [from *Zhao and Dai*, 2015].

over the regions with decreasing soil moisture and sc_PDSI_pm. These three measures of aridity (soil moisture, sc_PDSI_pm, and P/PET) show consistent drying patterns. This increases our confidence in these aridity change patterns.

Runoff ratio (R/P) is a key parameter in hydrology. Figure 2.10d shows that this ratio would decrease slightly by 0.02–0.06 hundredths over northern mid- to high-latitude land areas, where precipitation increases faster than runoff (Fig. 2.9); whereas it would increase slightly or change little over low-latitudes and the Southern Hemisphere. Averaged over global (60°S-75°N) land areas, the global-mean runoff ratio increases by ~2% from about 1990 to 2010 when the global-mean P, ET, and R all increased rapidly (Fig. 2.11). Thereafter, however, the global-mean runoff ratio does not change significantly over the 21st century, as the global-land P, R, and ET show similar percentage increases of 4%–5% by the end of the 21st century under the RCP4.5 scenario. This is in contrast to the notion that runoff ratio may change due to increased heavy precipitation, drier surface, and higher water use efficiency by plants in a GHG-induced warmer climate. The interannual to multiyear variations in R are larger than those in P and E (Fig. 2.11). This can be explained by the approximate relationship among these terms that requires the percentage change for R to be much larger than that for P or E [*Zhao and Dai*, 2015].

2.4.2. Streamflow Changes in the 21st Century

As discussed in the introduction, many studies have shown that the mean and extreme flow rates are likely to increase for many of world's major rivers under GHG-induced global warming in the 21st century. Very recently, *Koirala et al.* [2014] used a high-resolution (15') river routing model forced by daily runoff fields from 11 CMIP5 models under a high emissions (RCP8.5) scenario to simulate future streamflow changes. Figure 2.12 shows their 11 model ensemble-averaged percentage changes from 1971–2000 to 2071–2100 in the mean (Q_m), daily high (Q_5, top 5 percentiles) and low (Q_{95}, bottom 5 percentiles) streamflow flow rates. It is clear that the mean streamflow changes are broadly comparable to the total runoff changes (Fig. 2.9d) simulated directly by the CMIP5 models with coarser resolution. Figure 2.12a shows that mean streamflow (Q_m) would increase by 5%–80% over most of Asia (40%–80% in northeastern and South Asia), northern Europe (10%–30%), northern (20%–40%) and eastern (10%–30%) North America, central (10%–30%) and eastern (50%–80%) Africa, southeastern (30%–60%) and northwestern (10%–20%) South America, and central (40%–60%) and northern (5%–20%) Australia; but decrease by 5%–50% over southern Europe (10%–30%), northern Africa (5%–30%) and other regions around the Black and Caspian seas (15%–50%), southwestern North America (15%–35%)

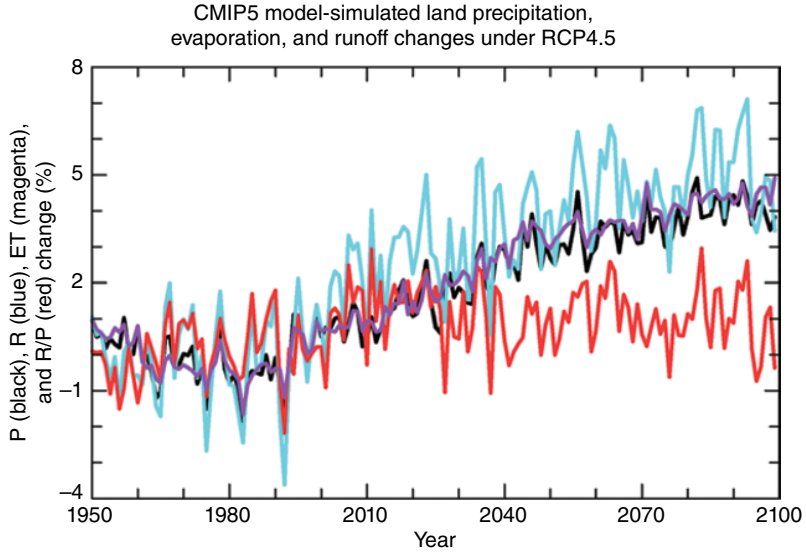

Figure 2.11 Time series of the changes (in percentage of the 1950–1979 mean) in globally (60°S–75°N) averaged land annual precipitation (P, black line), total runoff (R, blue), evapotranspiration (ET, magenta), and runoff ratio (R/P, red). The 1950–1979 mean for the global land P, R, ET, and R/P are 2.340, 0.709, 1.690, and 0.303, respectively [from *Zhao and Dai*, 2015].

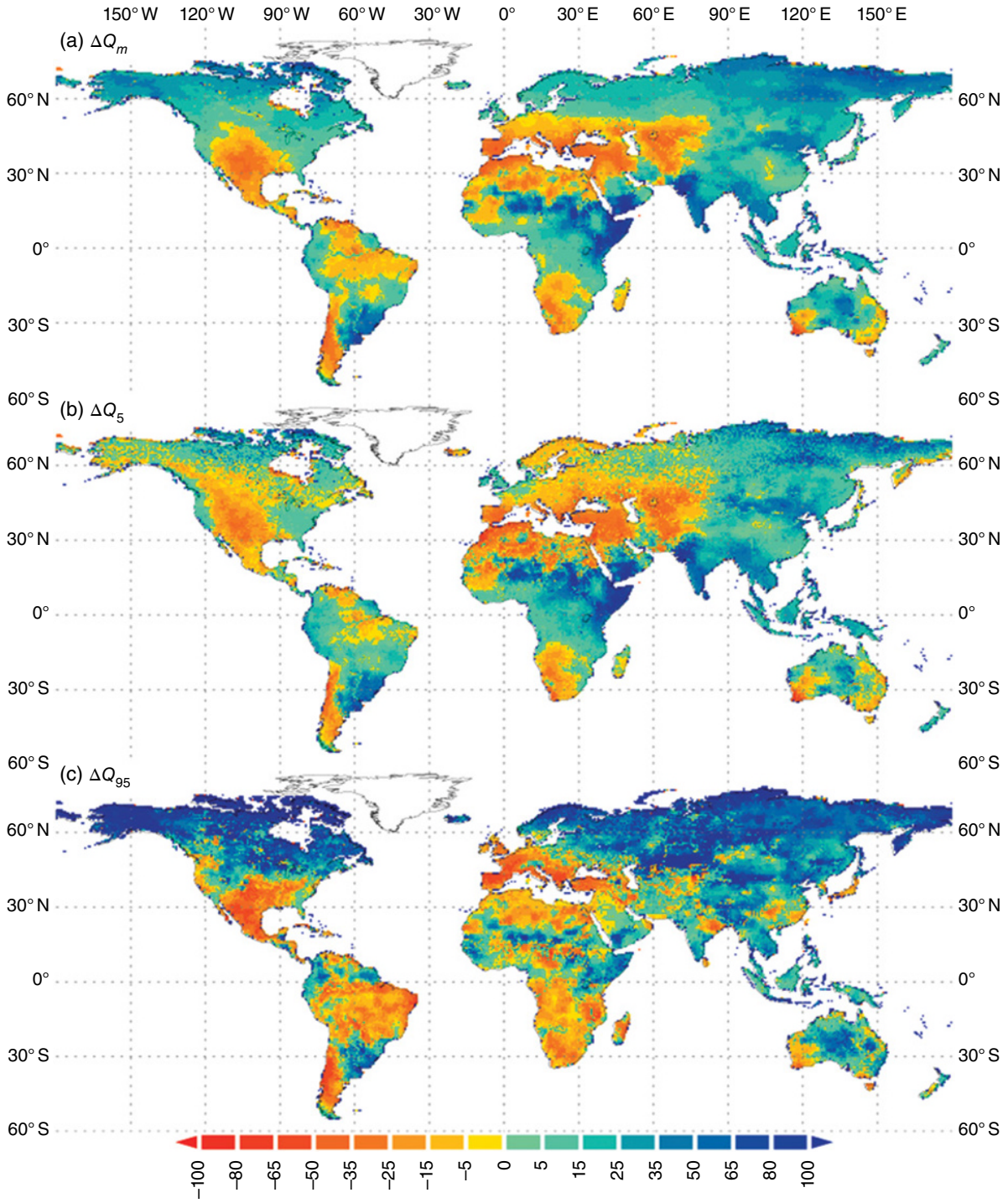

Figure 2.12 Relative change (difference of future [2071–2100] and past [1971–2000], divided by past) in percentage of multimodel means of (a) long-term mean stream flow (Qm), (b) high flow (Q5), and (c) low flow (Q95) under the RCP8.5 scenario. The flow rates were simulated by a high-resolution river routing model forced by the daily runoff fields from 11 CMIP5 models, and the simulated flow rates were then averaged to derive the multimodel mean shown here [from *Koirala et al.*, 2014, used with permission].

and Central America (5%–25%), most of northern (5%–20%) and southern (20%–40%) South America, southern Africa (10%–30%), and southwestern (10%–30%) and southeastern (5%–15%) coastal Australia. The percentage changes for the high flow rate (Q_5) roughly follow those for the mean flow rate with similar magnitudes, except for central and northern Europe and southern Canada, where the high flow rate decreases while the mean rate increases. The high flow rate also increases over most northern South America, in contrast to the decreases in the mean flow rate.

Figure 2.12c shows that the low flow rate would change at much larger percentage rates than the mean and high flow rates, partly due to its smaller mean values. The increases in the low flow rate over most Eurasia (except southern Europe) and North America (except its Southwest) are particularly large, ranging from 50% to over 100%. The decreases over southern Europe, southwestern North America and Central America, and southern and central South America range from 15% to 65% (Fig. 12c).

Similar to the runoff change (Fig. 2.9d), the consistency of the projected streamflow changes among the CMIP5 models is low over many land areas, except for the northern high latitudes, South Asia, East Africa, southern Europe, southwestern North America, and southern South America, where the consistency is high [*Koirala et al.*, 2014]. Furthermore, the intermodel consistency is higher for the changes in the low flow rate than for the mean and high flow rates [*Koirala et al.*, 2014], partly due to its larger magnitude of change. This is expected because realization-dependent internal variability can contribute to the decadal-mean changes projected by the models and overshadow the weak forced signal over many regions. Under the moderate emissions scenario RCP4.5, the projected changes in the streamflow rates show similar spatial patterns but with reduced magnitudes (~1/2 of Fig. 2.12), with the low flow rate still showing larger changes than the mean and high flow rates [*Koirala et al.*, 2014]. One exception is over central and northern Australia, where the streamflow increase seen under the RCP8.5 (Fig. 2.12) is less clear under the RCP4.5, consistent with the runoff changes shown in Fig. 2.9d.

2.5. SUMMARY

Streamflow and continental runoff represent the renewable freshwater resource to human society and other inhabitants on land. Thus, their variations and long-term changes are of great concern to us. While runoff is difficult to measure directly, streamflow over most of world's major rivers has been monitored by stream gauges for many decades, but recent streamflow data for many rivers in Asia and Africa are not made public and this hampers scientific research. More international efforts are needed to collect and compile streamflow data for scientific research.

An update of *Dai et al.* [2009] using available streamflow data from the world's 264 largest rivers shows that long-term (1948–2012) streamflow trends are statistically insignificant for most of the world's major rivers, although large multiyear to decadal variations are seen in these data. Out of the 200 largest rivers, only 55 (27.5%) show statistically significant trends, with negative trends (29) outnumbering positive trends (26). Global continental discharge exhibits large year-to-year variations, with a weak downward trend from 1949 to 1993; thereafter, it has increased to levels slightly above those from the 1950s to 1980s. Land precipitation generally follows these decadal changes, and it also correlates with the discharge on interannual to multiyear timescales. This increases our confidence in these two records that are physically related but independently measured.

Although the streamflow trends during 1948–2012 for most rivers are statistically insignificant individually, these trends show coherent spatial patterns that are broadly consistent with observed precipitation changes. These patterns show that from about 1950 to 2012, precipitation and runoff have decreased over most of Africa, East and South Asia, eastern coastal Australia, the southeast and northwest United States, western and eastern Canada, and parts of Brazil; but increased over Argentina and Uruguay, central and northern Australia, the central and northeast United States, central and northern Europe, and most of Russia. A large part of these regional trends likely has resulted from multidecadal internal climate variations, especially the Interdecadal Pacific Oscillation [IPO, *Dai,* 2013b; *Dong and Dai*, 2015], although the effect of global warming is likely also important [*Gu and Adler*, 2013]. On multiyear timescales, Pacific SSTs (namely ENSO) also have a large influence on continental discharge and precipitation, with low (high) land precipitation and continental runoff during El Niño (La Niña) events.

CMIP5 models generally predict increased precipitation (by 10%–25%) and runoff (by 5%–20%) in the 21st century under the moderate emissions scenario RCP4.5 over most of Asia, northern Europe, North America (except its Southwest), eastern Africa, and southwestern South America, but decreased precipitation and runoff (by 5%–15%) over southern Europe, northern and southern Africa, southwestern North America, Central America, and northern South America. Over Australia, precipitation is projected to decrease but runoff changes little. Runoff ratio decreases slightly in the northern mid- to high latitudes but changes littler in the low latitudes, resulting in no trends in global-mean runoff ratio during the 21st century.

Mean streamflow rates simulated by an off-line high-resolution river routing model [*Koirala et al*., 2014] forced by daily runoff output from the CMIP5 models show similar change patterns under a high (RCP8.5) and a moderate (RCP4.5) emissions scenario, and they are comparable to the runoff change patterns directly from the CMIP5 models. Under the RCP8.5 high emissions scenario in the 21st century, daily mean streamflow is projected to increase by 5%–80% over most of Asia, northern Europe, northern and eastern North America, central and eastern Africa, southeastern and northwestern South America, and central and northern Australia; but decrease by 5%–50% over southern Europe, northern Africa and other regions around the Black and Caspian Seas, southwestern North America and Central America, most of northern and southern South America, southern Africa, and southwestern and southeastern coastal Australia.

Changes for high streamflow rates roughly follow those for the mean flow rate with similar magnitudes, except for central and northern Europe and southern Canada, where the high flow rate decreases while the mean rate increases. Percentage changes in low streamflow rates are much larger than those for the mean and high flow rates, with more widespread decreases in Africa and South America but more increases in western Asia and central Europe.

The intermodel spread in the projected runoff and streamflow changes is large, and the consistency of the sign of change among the CMIP5 models is low over most areas except the northern high latitudes, South Asia and East Africa, southern Europe, southwestern North America, and southern South America, where the magnitude of change is large, which leads to high consistency among the models. A large part of the intermodel spread likely results from realization-dependent internal variability that is not related to differences in model physics.

ACKNOWLEDGMENTS

The author thanks Ulrich Looser and Thomas de Couet of GRDC for providing their updated streamflow data and granting permission for me to use Figures 2.1–2.2. The author also acknowledges the funding support from the National Science Foundation (NSF) (Grant No. AGS-1353740) and the U.S. Department of Energy's Office of Science (Award No. DE-SC0012602).

REFERENCES

Adam, J. C., A. F. Hamlet, and D. P. Lettenmaier (2009), Implications of global climate change for snowmelt hydrology in the twenty-first century, *Hydrol. Processes*, *23*, 962–972.

Adam, J. C., and D. P. Lettenmaier (2008), Application of new precipitation and reconstructed streamflow products to streamflow trend attribution in northern Eurasia, *J. Climate*, *21*, 1807–1828.

Alkama, R., B. Decharme, H. Douville, and A. Ribes (2011), Trends in global and basin-scale runoff over the late twentieth century: methodological issues and sources of uncertainty, *J. Climate*, *24*, 3000–3014. doi: http://dx.doi.org/10.1175/2010JCLI3921.1

Alkama, R., L. Marchand, A. Ribes, and B. Decharme (2013), Detection of global runoff changes: Results from observations and CMIP5 experiments, *Hydrol. Earth Syst. Sci. Discuss.*, *10*, 2117–2140.

Arnell, N. W., and B. Lloyd-Hughes (2014), The global-scale impacts of climate change on water resources and flooding under new climate and socio-economic scenarios, *Clim. Change.*, *122*, 127–140.

Arnell, N. W., and S. N. Gosling (2013), The impacts of climate change on river flow regimes at the global scale, *J. Hydrol.*, *486*, 351–364.

Baumgartner, A., and E. Reichel (1975), *The World Water Balance*, Elsevier.

Biemans, H., I. Haddeland, P. Kabat, F. Ludwig, R. W. A. Hutjes, J. Heinke, W. von Bloh, and D. Gerten (2011), Impact of reservoirs on river discharge and irrigation water supply during the 20th century, *Water Resour. Res.*, *47*, W03509, doi:10.1029/2009WR008929.

Birsan, M. V., P. Molnar, P. Burlando, and M. Pfaundler (2005), Streamflow trends in Switzerland, *J. Hydrol.*, *314*, 312–329.

Bodo, B. A. (2001), Annotations for monthly discharge data for world rivers (excluding former Soviet Union), 85 pp. [Available on-line from http://rda.ucar.edu/data sets/ds552.1/]

Bogardi, J. J., B. M. Fekete, and C. J. Vörösmarty (2013), Planetary boundaries revisited: a view through the 'water lens', *Current Opinion in Environmental Sustainability*, *5*, 581–589.

Boyer, E. W., R. W. Howarth, J. N. Galloway, F. J. Dentener, P. A. Green, and C. J. Vörösmarty (2006), Riverine nitrogen export from the continents to the coasts, *Glob. Biogeochem. Cycles*, *20*, GB1S91, doi:10.1029/2005GB002537.

Carton, J. A. (1991), Effect of seasonal surface fresh-water flux on sea-surface temperature in the tropical Atlantic Ocean, *J. Geophys. Res.*, *96*, 12593–12598.

Cayan, D. R., S. A. Kammerdiener, M. D. Dettinger, J. M. Caprio, and D. H. Peterson (2001), Changes in the onset of spring in the western United States, *Bull. Amer. Meteor. Soc.*, *82*, 399–415.

Chou, C., J. D. Neelin, C.-A. Chen, and J.-Y. Tu (2009), Evaluating the "rich-get-richer" mechanism in tropical precipitation change under global warming, *J. Climate*, *22*, 1982–2005.

Clark, E. A., J. Sheffield, M. T. H. van Vliet, B. Nijssen, and D. P. Lettenmaier (2015), Continental runoff into the oceans (1950–2008), *J. Hydrometeor*., *16*(4), 1502–1520.

Cluis, D., and C. Laberge (2001), Climate change and trend detection in selected rivers within the Asia-Pacific region, *Water Int.*, *26*, 411–424.

Collins, M., et al. (2013), Long-term climate change: Projections, commitments and irreversibility, in *Climate Change 2013:*

The Physical Science Basis, Contribution of Working Group I to the Fifth Assessment Report of the Intergovernmental Panel on Climate Change, edited by T. F. Stocker et al., Cambridge University Press, pp. 1029–1136.

Cook, B. I., J. E. Smerdon, R. Seager, and S. Coats (2014), Global warming and 21st century drying, *Climate Dyn.*, *43*, 2607–2627.

Cowell, C. M., and R. T. Stoudt (2002), Dam-induced modifications to upper Allegheny River streamflow patterns and their biodiversity implications, *J. Amer. Water Resour. Assoc.*, *38*, 187–196.

Dai, A. (2011a), Drought under global warming: A review, *Wiley Interdisc. Rev. Climate Change*, *2*, 45–65, doi:10.1002/wcc.81.

Dai, A. (2011b), Characteristics and trends in various forms of the Palmer Drought Severity Index (PDSI) during 1900–2008. *J. Geophys. Res.*, *116*, D12115, doi:10.1029/2010JD015541.

Dai, A. (2013a), Increasing drought under global warming in observations and models, *Nature Climate Change*, *3*, 52–58, doi:10.1038/nclimate1633.

Dai, A. (2013b), The influence of the Inter-decadal Pacific Oscillation on U.S. precipitation during 1923–2010, *Climate Dyn.*, *41*, 633–646, doi:10.1007/s00382-012-1446-5.

Dai, A., and K. E. Trenberth (2002), Estimates of freshwater discharge from continents: Latitudinal and seasonal variations, *J. Hydrometeor.*, *3*, 660–687.

Dai, A., and T. M. L. Wigley (2000), Global patterns of ENSO-induced precipitation, *Geophys. Res. Lett.*, *27*, 1283–1286.

Dai, A., T. T. Qian, K. E. Trenberth, and J. D. Milliman (2009), Changes in continental freshwater discharge from 1948 to 2004, *J. Climate*, *22*, 2773–2792.

Dankers R and L Feyen (2009), Flood hazard in Europe in an ensemble of regional climate scenarios. *J. Geophys. Res. 114* D16108, doi: 10.1029/2008JD011523.

Dankers, R., et al (2014), First look at changes in flood hazard in the inter-sectoral impact model intercomparison project ensemble, *Proc. Nat. Acad. Sci.*, *111*, 3257–3261.

Davie, J. C. S., et al. (2013), Comparing projections of future changes in runoff and water resources from hydrological and ecosystem models in ISI-MIP, *Earth Syst. Dynam. Discuss.*, *4*, 279–315, doi:10.5194/esdd-4-279-2013.

Dettinger, M. D., and H. F. Diaz (2000), Global characteristics of stream flow seasonality and variability, *J. Hydrometeor.*, *1*, 289–310.

Döll, P., F. Kaspar, and B. Lehner (2003), A global hydrological model for deriving water availability indicators: Model tuning and validation, *J. Hydrol.*, *270*, 105–134.

Döll, P., K. Fiedler, and J. Zhang (2009), Global-scale analysis of river flow alterations due to water withdrawals and reservoirs, *Hydrol. Earth Syst.Sci.*, *13*(12), 2413–2432, doi:10.5194/hess-13-2413-2009.

Döll, P., and H. M. Schmied (2012), How is the impact of climate change on river flow regimes related to the impact on mean annual runoff? A global-scale analysis, *Environ. Res. Lett.*, *7*, doi:10.1088/1748-9326/7/1/014037.

Dong, B., and A. Dai (2015), The influence of the Inter-decadal Pacific Oscillation on temperature and precipitation over the globe, *Climate Dyn.*, *45*, 2667–2681, doi:10.1007/s00382-015-2500-x.

Espinoza Villar, J. C., et al. (2009), Contrasting regional discharge evolutions in the Amazon basin (1974–2004), *J. Hydrol.*, *375*, 297–311.

Fekete, B., C. J. Vörösmarty, and W. Grabs (2000), *Global Composite Runoff Fields Based on Observed Discharge and Simulated Water Balances*. Global Runoff Data Centre Rep. No.22. Federal Institute of Hydrology (BfG), 108 pp.

Fekete, B. M., C. J. Vörösmarty, and W. Grabs (2002), High-resolution fields of global runoff combining observed river discharge and simulated water balances, *Glob. Biogeochem. Cycles*, *16*, 1042, doi:10.1029/1999GB001254.

Feng, S., and Q. Fu (2013), Expansion of global drylands under warming climate, *Atmos. Chem. Phys.*, *13*, 10081–10094.

Gedney, N., P. M. Cox, R. A. Betts, O. Boucher, C. Huntingford, and P. A. Stott (2006), Detection of a direct carbon dioxide effect in continental river runoff records, *Nature*, *439*, 835–838.

Genta, J. L., G. Perez-Iribarren, and C. R. Mechoso (1998), A recent increasing trend in the streamflow of rivers in southeastern South America, *J. Climate*, *11*, 2858–2862.

Giuntoli, I., B. Renard, J. P. Vidal, and A. Bard (2013), Low flows in France and their relationship to large-scale climate indices, *J. Hydrol.*, *482*, 105–118.

Global Runoff Data Centre (2013), Long-Term Mean Monthly Discharges and Annual Characteristics of GRDC Station/Global Runoff Data Centre, Federal Institute of Hydrology (BfG), Koblenz, Germany. [Available at http://www.bafg.de/GRDC/EN.]

Grabs, W. E., F. Portmann, and T. de Couet (2000), Discharge observation networks in Arctic regions: Computation of the river runoff into the Arctic Ocean, its seasonality and variability, in *The Freshwater Budget of the Arctic Ocean*, edited by E. L. Lewis et al., pp. 249–267, Kluwer Academic Publ., Dordrecht.

Grabs, W. E., T. de Couet, and J. Pauler (1996), Freshwater fluxes from continents into the world oceans based on data of the global runoff data base. Global Runoff Data Centre (GRDC) Rep. No. 10, Germany, 49 pp. + annex 179 pp. [Available from GRDC, Fed. Inst. of Hydrology, Kaiserin-Augusta-Anlagen 15-17, D-56068 Koblenz, Germany]

Groisman, P., R. Knight, T. R. Karl, D. Easterling, B. M. Sun, and J. Lawrimore (2004), Contemporary changes of the hydrological cycle over the contiguous United States: Trends derived from in situ observations, *J. Hydrometeor.*, *5*, 64–85.

Groisman, P. Y., R. W. Knight, and T. R. Karl (2001), Heavy precipitation and high streamflow in the contiguous United States: Trends in the twentieth century, *Bull. Amer. Meteor. Soc.*, *82*, 219–246.

Gu, G., and R. F. Adler (2013), Interdecadal variability/long-term changes in global precipitation patterns during the past three decades: global warming and/or pacific decadal variability? *Climate Dyn.*, *40*, 3009–3022.

Guetter, A. K., and K. P. Georgakakos (1993), River Outflow of the Conterminous United-States, 1939–1988, *Bull. Amer. Meteor. Soc.*, *74*, 1873–1891.

Haddeland, I., et al. (2014), Global water resources affected by human interventions and climate change, *Proc. Nat. Acad. Sci.*, *111*, 3251–3256.

Hannah, D. M., S. Demuth, H. A. J. van Lanen, U. Looser, C. Prudhomme, G. Rees, K. Stahl, and L. M. Tallaksen (2011), Large-scale river flow archives: importance, current status and future needs, *Hydrolog. Processes*, *25*, 1191–1200.

Hegerl, G. C., et al. (2015), Challenges in quantifying changes in the global water cycle, *Bull. Amer. Meteor. Soc.*, *96*, 1097–1115.

Hirabayashi, Y., S. Kanae, S. Emori, T. Oki, and M. Kimoto (2008), Global projections of changing risks of floods and droughts in a changing climate, *Hydrol. Sci. J.*, *53*, 754–72.

Hirabayashi, Y., R. Mahendran, S. Koirala, L. Konoshima, D. Yamazaki, S. Watanabe, H. Kim, and S. Kanae (2013), Global flood risk under climate change, *Nature Climate Change.*, *3*, 816–21.

Hodgkins, G. A., R. W. Dudley, and T. G. Huntington (2003), Changes in the timing of high river flows in New England over the 20th Century, *J. Hydrol.*, *278*, 244–252.

Huffman, G. J., R. F. Adler, D. T. Bolvin, and G. Gu (2009), Improving the global precipitation record: GPCP version 2.1, *Geophys., Res., Lett.*, *36*, L17808, doi:10.1029/2009GL040000.

Hyvärinen, V. (2003), Trends and characteristics of hydrological time series in Finland, *Nordic Hydrol.*, *34*, 71–90.

Koirala, S., Y. Hirabayashi, R. Mahendran, and S. Kanae (2014), Global assessment of agreement among streamflow projections using CMIP5 model outputs. *Environ. Res. Lett.*, *9*, 064017, doi:10.1088/1748-9326/9/6/064017.

Korzun, V. I. (1978), *World Water Balance and Water Resources of the Earth*. English translation, R. L. Nace, Ed., UNESCO, 663 pp.

Krepper, C. M., N. O. Garcia, and P. D. Jones (2006), Paraguay river basin response to seasonal rainfall, *Intl. J. Climatol.*, *26*, 1267–1278.

Kundzewicz, Z., N. Lugeri, R. Dankers, Y. Hirabayashi, P. Döll, I. Pińskwar, T. Dysarz, S. Hochrainer, and P. Matczak (2010), Assessing river flood risk and adaptation in Europe—review of projections for the future, *Mitig. Adapt. Strateg. Glob. Change*, *15*, 641–656.

Labat, D. (2010), Cross wavelet analyses of annual continental freshwater discharge and selected climate indices, *J. Hydrol.*, *385*, 269–278.

Labat, D., Y. Goddéris, J. L. Probst, and J. L. Guyot (2004), Evidence for global runoff increase related to climate warming, *Adv. Water Resour.*, *27*, 631–642.

Lammers, R. B., A. I. Shiklomanov, C. J. Vorosmarty, B. M. Fekete, and B. J. Peterson (2001), Assessment of contemporary Arctic river runoff based on observational discharge records, *J. Geophys. Res. Atmos.*, *106*, 3321–3334.

Legates, D. R., H. F. Lins, and G. J. McCabe (2005), Comments on "Evidence for global runoff increase related to climate warming" by Labat et al., *Adv. Water Resour.*, *28*, 1310–1315.

Lettenmaier, D. P., E. F. Wood, and J. R. Wallis (1994), Hydro-climatological trends in the continental United States, 1948–88, *J. Climate*, *7*, 586–607.

Lindstrom, G., and S. Bergstrom (2004), Runoff trends in Sweden 1807–2002, *Hydrol. Sci. J.*, *49*, 69–83.

Lins, H. F., and J. R. Slack (1999), Streamflow trends in the United States, *Geophys. Res. Lett.*, *26*, 227–230.

Lu, J., G. A. Vecchi, and T. J. Reichler (2007), Expansion of the Hadley cell under global warming, *Geophys. Res. Lett.*, *34*, L06805, doi:10.1029/2006GL028443.

L'vovich, M. I. (1979), *World Water Resources and Their Future*, American Geophysical Union.

Marcinek, J. (1964), The River Discharge from Land Surface over the Globe and its Distribution in 5° Zones (in German), *Bull. Inst. Water Man.*, *21*, 204 pp.

McCabe, G. J., and D. M. Wolock (2011), Century-scale variability in global annual runoff examined using a water balance model, *Int. J. Climatol.*, *31*, 1739–1748.

Meehl, G. A., T. F. Stocker, W. D. Collins, P. Friedlingstein, A. T. Gaye, et al. (2007), Global climate projections, *Climate Change 2007: The Physical Science Basis. Contribution of Working Group I to the Fourth Assessment Report of the IPCC*, edited by S. Solomon et al., Cambridge University Press, pp. 746–845.

Milliman, J. D., K. L. Farnsworth, P. D. Jones, K. H. Xu, and L. C. Smith (2008), Climatic and anthropogenic factors affecting river diSchärge to the global ocean, 1951–2000, *Global Planet. Change*, *62*, 187–194.

Milly, P. C. D., R. T. Wetherald, K. A. Dunne, and T. L. Delworth (2002), Increasing risk of great floods in a changing climate, *Nature*, *415*, 514–517.

Milly, P. C. D., K. A. Dunne, and A. V. Vecchia (2005), Global pattern of trends in streamflow and water availability in a changing climate, *Nature*, *438*, 347–350.

Munier1, H. P., P. Maisongrande, A. Cazenave, and E. F. Wood (2012), Global runoff over 1993–2009 estimated from coupled land-ocean-atmosphere water budgets and its relation with climate variability, *Hydrol. Earth Syst. Sci. Discuss.*, *9*, 4633–4665.

Nijssen, B. N., G. M. O'Donnell, D. P. Lettenmaier, and E. F. Wood (2001), Predicting the discharge of global rivers, *J. Climate*, *14*, 3307–3323.

Nilsson, C., C. A. Reidy, M. Dynesius, and C. Revenga (2005), Fragmentation and flow regulation of the world's large river systems, *Science*, *308*, 405–408.

Nohara, D., A. Kitoh, M. Hosaka, and T. Oki (2006), Impact of climate change on river discharge projected by multimodel ensemble, *J. Hydrometeor.*, *7*, 1076–1089.

Oki, T., and S. Kanae (2006), Global hydrological cycles and world water resources, *Science*, *313*, 1068–1072.

Oki, T., Y. Agata, S. Kanae, T. Saruhashi, D. Yang, and K. Musiake (2001), Global assessment of current water resources using total runoff integrated pathways, *Hydrol. Sci. J.*, *46*, 983–995.

Pasquini, A. I., and P. J. Depetris (2007), Discharge trends and flow dynamics of South American rivers draining the southern Atlantic seaboard: An overview, *J. Hydrol.*, *333*, 385–399.

Peel, M. C., and T. A. McMahon (2006), Continental runoff - A quality-controlled global runoff data set, *Nature*, *444*, E14–E14.

Pekárová, P., P. Miklánek, and J. Pekár (2003), Spatial and temporal runoff oscillation analysis of the main rivers of the world during the 19th–20th centuries, *J. Hydrol.*, *274*, 62–79.

Perry, G. D., P. B. Duffy, and N. L. Miller (1996), An extended data set of river discharges for validation of general circulation models, *J. Geophys. Res.*, *101*, 21339–21349.

Peterson, B. J., R. M. Holmes, J. W. McClelland, C. J. Vörösmarty, R. B. Lammers, A. I. Shiklomanov, I. A. Shiklomanov, and S. Rahmstorf (2002), Increasing river discharge to the Arctic Ocean, *Science*, *298*, 2171–2173.

Piao, S., et al. (2010), The impacts of climate change on water resources and agriculture in China, *Nature*, *467*, 43–51.

Piao, S., P. Friedlingstein, P. Ciais, N. de Noblet-Ducouvré, D. Labat, and S. Zaehle (2007), Climate and land-use change have a larger impact than rising CO2 on global river runoff trends, *PNAS*, *104*, 15242–15247.

Probst, J. L., and Y. Tardy (1987), Long-Range Streamflow and World Continental Runoff Fluctuations since the Beginning of This Century, *J. Hydrol.*, *94*, 289–311.

Probst, J. L., and Y. Tardy (1989), Global Runoff Fluctuations During the Last 80 Years in Relation to World Temperature-Change, *Amer. J. Sci.*, *289*, 267–285.

Prudhomme, C., et al. (2014), Hydrological droughts in the 21st century, hotspots and uncertainties from a global multimodel ensemble experiment, *PNAS*, *111*, 3262–3267.

Qian, T., A. Dai, K. E. Trenberth, and K. W. Oleson (2006), Simulation of global land surface conditions from 1948–2004. Part I: Forcing data and evaluation, *J. Hydrometeor.*, *7*, 953–975.

Qian, T., A. Dai, and K. E. Trenberth (2007), Hydroclimatic trends in the Mississippi River basin from 1948–2004, *J. Climate*, *20*, 4599–4614.

Rawlins, M. A., C. J. Willmott, A. Shiklomanov, E. Linder, S. Frolking, R. B. Lammers, and C. J. Vörösmarty (2006), Evaluation of trends in derived snowfall and rainfall across Eurasia and linkages with discharge to the Arctic Ocean. *Geophys. Res. Lett.*, *33*, L07403, doi:10.1029/2005GL025231.

Robson, A. J. (2002), Evidence for trends in UK flooding, *Philosophical Transactions of the Royal Society of London A: Mathematical Physical and Engineering Sciences*, *360*, 1327–1343.

Rodell, M., P. R. Houser, U. Jambor, J. Gottschalck, K. Mitchell, C.-J. Meng, K. Arsenault, B. Cosgrove, J. Radakovich, M. Bosilovich, J. K. Entin, J. P. Walker, D. Lohmann, and D. Toll (2004), The Global Land Data Assimilation System, *Bull. Amer. Meteor. Soc.*, *85*(3), 381–394.

Scheff, J., and D. M. W. Frierson (2012), Robust future precipitation declines in CMIP5 largely reflect the poleward expansion of model subtropical dry zones, *Geophys. Res. Lett.*, *39*, L18704, doi:10.1029/2012GL052910.

Scheff, J, and D. M. W. Frierson (2014), Scaling Potential Evapotranspiration with Greenhouse Warming. *J. Climate*, *27*, 1539–1558.

Schewe, J., et al. (2014), Multimodel assessment of water scarcity under climate change, *PNAS*, *111*, 3245–3250.

Schneider, U., A. Becker, P. finger, A. Meyer-Christoffer, M. Ziese, and B. Rudolf (2014), GPCC's new land surface precipitation climatology based on quality-controlled in situ data and its role in quantifying the global water cycle, *Theor. Appl. Climatol.*, *115*, 15–40.

Sheffield, J., and E. F. Wood (2008), Projected changes in drought occurrence under future global warming from multi-model, multi-scenario, IPCC AR4 simulations, *Climate Dyn.*, *31*, 79–105.

Shiklomanov, A. I., R. B. Lammers, and C. J. Vörösmarty (2002), Widespread decline in hydrological monitoring threatens pan-Arctic research, *Eos, Trans. Amer. Geophys. Union*, *83*, 13–16.

Shiklomanov, A. I., R. B. Lammers, M. A. Rawlins, L. C. Smith, and T. M. Pavelsky (2007), Temporal and spatial variations in maximum river discharge from a new Russian data set, *J. Geophys. Res. Biogeosci.*, *112*, G04S53.

Shiklomanov, A. I., T. I. Yakovleva, R. B. Lammers, I. P. Karasev, C. J. Vörösmarty, and E. Linder (2006), Cold region river discharge uncertainty - estimates from large Russian rivers, *J. Hydrol.*, *326*, 231–256.

Shuttleworth, W. J. (1993), Evaporation, in *Handbook of Hydrology*, edited by D. R. Maidment, pp. 4.1–4.53, McGraw-Hill, New York.

Smith, L. C. (2000), Trends in Russian Arctic river-ice formation and breakup: 1917 to 1994, *Phys. Geogr.*, *21*, 46–56.

Stahl, K., et al. (2010), Streamflow trends in Europe: Evidence from a data set of near-natural catchments, *Hydrol. Earth Syst. Sci.*, *14*, 2367–2382.

Sun, Y., S. Solomon, A. Dai, and R. Portmann (2007), How often will it rain? *J. Climate*, *20*, 4801–4818.

Syed, T. H., J. S. Famiglietti, and D. P. Chambers (2009), GRACE-based estimates of terrestrial freshwater discharge from basin to continental scales, *J. Hydrometeor.*, *10*, 22–40.

Syed, T. H., J. S. Famiglietti, D. P. Chambers, J. K. Willis, and K. Hilburn (2010), Satellite-based global-ocean mass balance estimates of interannual variability and emerging trends in continental freshwater discharge, *PNAS*, *107*, 17916–17921.

Tang, Q. H., and Lettenmaier, D. P. (2012), 21st century runoff sensitivities of major global river basins. *Geophys. Res. Lett. 39*, L06403, doi:10.1029/2011GL050834.

Trenberth, K. E., A. Dai, R. M. Rasmussen, and D. B. Parsons (2003), The changing character of precipitation, *Bull. Amer. Met. Soc.*, *84*, 1205–1217.

Trenberth, K. E., and A. Dai (2007), Effects of Mount Pinatubo volcanic eruption on the hydrological cycle as an analog of geoengineering. *Geophys. Res. Lett.*, *34*, L15702, doi:10.1029/2007GL030524.

Trenberth, K. E., L. Smith, T. Qian, A. Dai, and J. Fasullo (2007), Estimates of the global water budget and its annual cycle using observational and model data, *J. Hydrometeor.*, *8*, 758–769.

van Vliet, M. T. H., W. H. P. Franssena, J. R. Yearsley, F. Ludwig, I. Haddeland, D. P. Lettenmaier, and P. Kabat (2013), Global river discharge and water temperature under climate change, *Global Environ. Change*, *23*, 450–464.

Vörösmarty, C. J., P. Green, J. Salisbury, and R. B. Lammers (2000), Global water resources: Vulnerability from climate change and population growth, *Science*, *289*, 284–288.

Wada, Y., L. P. H. van Beek, C. M. van Kempen, J. W. T. M. Reckman, S. Vasak, and M. F. P. Bierkens (2010), Global depletion of groundwater resources, *Geophys. Res. Lett.*, *37*, L20402, doi:10.1029/2010GL044571.

Wang, G. L. (2005), Agricultural drought in a future climate: Results from 15 global climate models participating in the IPCC 4th assessment, *Climate Dyn.*, *25*, 739–753.

Wilkinson, K., M. von Zabern, and J. Scherzer (2014), Global Freshwater Fluxes into the World Oceans. Tech. Report prepared for the GRDC. - Koblenz, Federal Institute of Hydrology (BfG), (GRDC Report No. 44. doi: 10.5675/GRDC_Report_44, 23pp. [Available from http://www.bafg.de/GRDC/EN/02_srvcs/24_rprtsrs/report_44.pdf]

Xiong, L. H., and S. L. Guo (2004), Trend test and change-point detection for the annual discharge series of the Yangtze River at the Yichang hydrological station, *Hydrol. Sci. J.*, *49*, 99–112.

Yang, D., B. Ye, and D. L. Kane (2004a), Streamflow changes over Siberian Yenisei River Basin, *J. Hydrol.*, *296*, 59–80.

Yang, D. Q., B. S. Ye, and A. Shiklomanov (2004b), Discharge characteristics and changes over the Ob River watershed in Siberia, *J. Hydrometeor.*, *5*, 595–610.

Ye, B. S., D. Q. Yang, and D. L. Kane (2003), Changes in Lena River streamflow hydrology: Human impacts versus natural variations, *Water Resour. Res.*, *39*, 1200, doi:10.1029/2003WR001991.

Zhang, X., J. He, J. Zhang, I. Polaykov, R. Gerdes, J. Inoue, and P. Wu (2012), Enhanced poleward moisture transport and amplified northern high-latitude wetting trend, *Nature Climate Change*, *3*, 47–51.

Zhang, X. B., F. W. Zwiers, G. C. Hegerl, F. H. Lambert, N. P. Gillett, S. Solomon, P. A. Stott, and T. Nozawa (2007), Detection of human influence on twentieth-century precipitation trends, *Nature*, *448*, 461–464.

Zhang, X. B., K. D. Harvey, W. D. Hogg, and T. R. Yuzyk (2001), Trends in Canadian streamflow, *Water Resour. Res.*, *37*, 987–998.

Zhao, T., and A. Dai (2015), The magnitude and causes of global drought changes in the 21st century under a moderate emissions scenario, *J. Climate*, *28*, 4490–4512.